Received: 5 August 2024 | Accepted: 3 February 2025

DOI: 10.1002/saj2.70028

Soil Science Society of America Journal

REVIEW

Fundamental Soil Science

Prediction accuracy of pXRF, MIR, and Vis-NIR spectra for soil properties—A review

Gafur Gozukara[1,2] | Alfred E. Hartemink[1] | Jingyi Huang[1] | José Alexandre Melo Demattê[3]

[1]FD Hole Soils Lab, Department of Soil Science, University of Wisconsin-Madison, Madison, Wisconsin, USA

[2]Department of Soil Science and Plant Nutrition, Eskisehir Osmangazi University, Eskisehir, Türkiye

[3]Department of Soil Science, College of Agriculture Luiz de Queiroz, University of São Paulo, Piracicaba, São Paulo, Brazil

Correspondence
Alfred E. Hartemink, Department of Soil Science, University of Wisconsin-Madison, FD Hole Soils Lab, 1525 Observatory Drive, Madison, WI 53706, USA.
Email: alfred.hartemink@wisc.edu

Assigned to Associate Editor Tetsuhiro Watanabe.

Abstract

Here, we review the prediction accuracy for soil properties using portable X-ray fluorescence (pXRF), mid-infrared (MIR), and visible near-infrared (Vis-NIR) and the factors impacting predictions and its accuracy. In total, 305 published papers were reviewed, and most of them were from Australia, Brazil, China, and the United States. About 44% of papers focused on the prediction of soil organic carbon (SOC) using Vis-NIR spectra. Partial least squares regression was most frequently used. Most studies sampled Alfisols, Inceptisols, and Entisols, and up to 40-cm depth. Researcher-based factors (type or brand of spectrometers, which differ in hardware, spectral range, resolution, and calibration protocols; preprocessing methods; prediction models; and soil analysis methods for calibration) and soil-based factors (horizon and depth) were explored. MIR spectra had better prediction accuracy with a mean R^2 over 0.8 for sand, clay, total N, total C (TC), SOC and soil inorganic carbon (SIC), and cation exchange capacity compared to Vis-NIR and pXRF. In the past 20 years, prediction accuracy tended to increase for sand, silt, clay, SIC, soil organic matter, and EC when using MIR and Vis-NIR spectra, and for TC and $CaCO_3$ when using pXRF spectra. Preprocessing methods, spectral range, calibration, type of the prediction models (i.e., machine and deep learning), and source of soil spectra (Vis-NIR, MIR, and pXRF), which are used to reduce noise and multicollinearity, calibrate data, and smooth spectra, all affected the prediction. In general, MIR spectra obtained the highest prediction accuracy for most soil properties. Future studies should focus on the effects of soil-based factors (parent material, soil mineralogy, pedogenesis, soil type, and horizon/depth) on the prediction accuracy of soil physical and chemical properties.

Abbreviations: BOC, baseline offset correction; CEC, cation exchange capacity; CNN, convolutional neural network; EC, electrical conductivity; EN, elastic net; Lasso, least absolute shrinkage and selection operator; MIR, mid-infrared; PLSR, partial least squares regression; pXRF, portable X-ray fluorescence; RF, random forest; SG, Savitzky–Golay; SIC, soil inorganic carbon; SOC, soil organic carbon; SOM, soil organic matter; SST, spectral space transformation; SVM, support vector machine; TC, total carbon; TN, total nitrogen; Vis-NIR, visible near-infrared.

1 | INTRODUCTION

Soil is a vital component of ecosystem functioning and one of the most intricate biomaterials on the planet (Young & Crawford, 2004). Soil is part of the terrestrial ecosystem that regulates the atmosphere, hydrosphere, biosphere, and lithosphere (Szabolcs, 1994). Monitoring and measuring its properties are needed to understand, manage, and quantify ecosystem services. Conventional physical and chemical analysis methods are costly and there is a demand for the fast, low-cost, sustainable, and nondestructive characterization of soil samples (Demattê et al., 2019a, 2019b; Duda et al., 2017; Gozukara, Acar et al., 2022; Terra et al., 2015).

Proximal sensors evaluate soil properties in a nondestructive condition (Viscarra Rossel et al., 2006). These sensors can provide information about soil characteristics such as soil moisture, texture, soil organic carbon (SOC), electrical conductivity (EC), pH, cation exchange capacity (CEC), mineralogy, and nutrient levels, which are needed for optimizing crop production, managing soil health, or environmental monitoring (Andrade, Silva, Weindorf et al., 2020; Gozukara, Altunbas et al., 2022; Levi et al., 2020). Among the relatively low-cost and easy-to-use proximal sensors, visible near-infrared (Vis-NIR) (350–2500 nm), mid-infrared (MIR) (2500–25,000 nm), and portable X-ray fluorescence (0–50 keV) spectroscopy have been used in soil science (Gozukara et al., 2021; Minasny et al., 2008, 2009; Stevenson et al., 2023; Zhang et al., 2022). Numerous studies have produced the relationships between the reflected energy of Vis-NIR, MIR, and pXRF and soil physical and chemical properties (Grinand et al., 2012; Naimi et al., 2022; O'Rourke, Minasny et al., 2016; O'Rourke, Stockmann et al., 2016; Ng et al., 2019, 2020; S. H. G. Silva et al., 2020).

The relationship between spectral reflectance and soil properties may vary depending on the spectral resolution and the soil sample characteristics (S. Liu et al., 2019; Nocita et al., 2014). The prediction accuracy is affected by different land use, climate conditions, parent material, soil types (Benedet et al., 2020; Mancini et al., 2020), depth/horizon (Andrade, Silva, Weindorf et al., 2020; Gozukara, Zhang et al., 2022; Zhao et al., 2021), and pedogenetic conditions (Demattê & Terra, 2014). Additionally, specific spectral characteristics can be related to specific chemical components (Padarian et al., 2019), but the accuracy is affected by the type of proximal sensor (Naimi et al., 2022; Raimo et al., 2022; Zhang & Hartemink, 2020), spectral range (Pirie et al., 2005; Raimo et al., 2022), spectral preprocessing methods (Dotto et al., 2017; Zhang & Hartemink, 2020), and the models used (Nawar et al., 2016; Ng et al., 2019; Padarian et al., 2019).

Previous reviews on soil spectroscopy have focused on the use of Vis-NIR (Ahmadi et al., 2021) or its combined use with MIR to compare the prediction performance, and in particular SOC and soil organic matter (SOM), EC (Bellon-Maurel & McBratney, 2011; Milinovic et al., 2023; Soriano-Disla et al., 2014; Viscarra Rossel et al., 2006). There is a need to understand the factors that affect the prediction performance and the relationship between soil and reflectance. Here, we review the prediction accuracy of Vis-NIR, MIR, and pXRF spectral information for soil properties and the factors that have impact on the results. We have reviewed this by analyzing the data from 305 papers related to the prediction of silt, clay, total nitrogen (TN), total carbon (TC), soil inorganic carbon (SIC), SOC, SOM, CEC, EC, pH, and $CaCO_3$ from soil spectroscopy and machine learning techniques.

Core Ideas

- The use of visible near-infrared, mid-infrared, and portable X-ray fluorescence spectra for predicting soil properties has exponentially increased.
- The accuracy of predicting sand, silt, clay, soil inorganic carbon, soil organic matter, electrical conductivity, total carbon, and $CaCO_3$ has increased over time.
- Prediction accuracy was affected by soil horizon, depth, type or brand of spectrometers, which differ in hardware, spectral range, resolution, and calibration protocols; prediction models; preprocessing; and soil analysis methods.

2 | DATA SOURCES

2.1 | Literature search

The Scopus database was used to collect primary research papers that applied Vis-NIR, MIR, and pXRF spectrometers for the characterization and prediction of the soil properties. We reviewed the years from 1992 to 2022, and excluded book chapters, reviews, and data papers. Some studies applied Vis-NIR, MIR, and pXRF spectra in the same paper, and therefore the number of papers used in this study was categorized individually. In total, 1006 Vis-NIR, 404 MIR, and 301 pXRF papers were selected from Scopus.

Papers were selected that focused on the prediction of physical and chemical soil properties (sand, silt, clay, TN, TC, SIC, SOC, SOM, CEC, EC, pH, and $CaCO_3$). On the other hand, very few studies used spectroscopy (Vis-NIR, MIR, and pXRF) to predict soil biological (Rasche et al., 2013; Soriano-Disla et al., 2014; Zhang et al., 2022) and mineralogical properties (Mendes et al., 2021; Rosin et al., 2023). Only studies that used data splitting as calibration and validation were selected; studies that used calibration procedures such as leave-one-out, *k*-fold, or repeated *k*-fold without data splitting strategies were not included. Studies that used the coefficient of determination (R^2) to test prediction accuracy were selected because it is commonly used among other accuracy criteria such as adjusted R^2, the squared Pearson correlation coefficient (r^2), root mean square error, the ratio of performance to deviation, and the ratio of performance to interquartile range.

From 257 (Vis-NIR), 70 (MIR), and 29 (pXRF) papers, data were extracted including soil properties, spectral range, sampling depth, number of soil samples, country, and soil type. Detailed information about the selected papers is given in Supporting Information 1 and 2. The R^2 value was extracted from the dependent validation dataset for each paper. Some papers had R^2 values for different soil types (soil taxonomy), parent materials, soil depths, horizons, spectral preprocessing methods, spectral ranges, and the types of Vis-NIR, MIR, and pXRF spectra.

A range of analytical methods were used for soil physical and chemical properties and, in particular, for the analysis of SOC and SOM. Several ratios, such as 1:1, 1:2, 1:2.5, and 1:5 of soil/water, KCl, or $CaCl_2$, were used to measure soil pH as well as EC.

The Tukey comparison test was applied with a significance level of $p \leq 0.05$ to compare the prediction accuracy of each spectrometer for soil physical and chemical properties. This analysis was conducted using the Minitab 19 statistics program (Minitab Inc.).

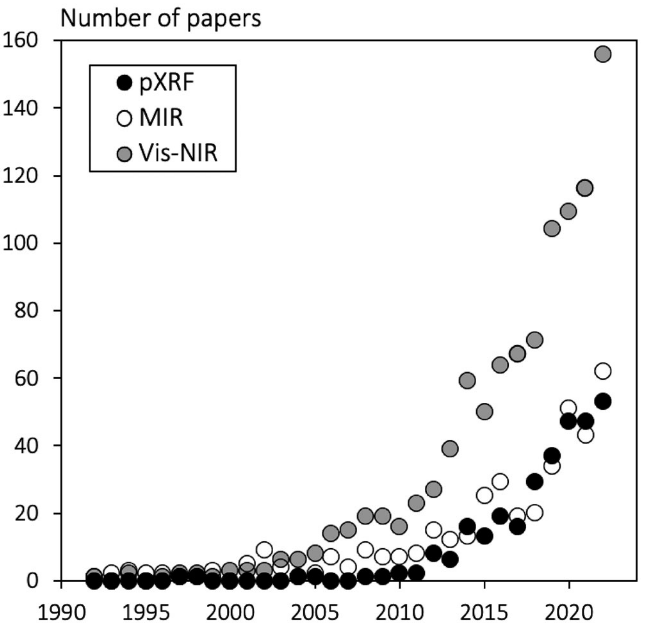

FIGURE 1 The number of papers per year for the characterization and prediction of soil properties using portable X-ray fluorescence (pXRF) ($n = 301$), mid-infrared (MIR) ($n = 404$), and visible near-infrared (Vis-NIR) ($n = 1006$) spectra. Data were extracted from papers in Scopus over the period 1992–2022, using the keywords "Vis-NIR or VNIR or VNir and Soil," "MIR or Mir and Soil," and "pXRF or p-XRF and Soil."

3 | RESULTS

3.1 | Origin of the research

The number of papers per year from January 1992 to December 2022 is shown in Figure 1. Since 2009, there has been a notable increase in papers for each spectrometer. The number of papers using pXRF increased from one paper in 2009 to 53 papers in 2022. Similarly, MIR-related studies increased from 15 to 90 papers (six times increase). Vis-NIR has seen the most substantial rise in number, with papers increasing from 30 in 2009 to over 150 in 2022 (five times increase). Thus, we see that Vis-NIR is the most widely used, while pXRF has the highest increase in ratio. This indicates that Vis-NIR is currently utilized about two to three times more than MIR and pXRF; many studies on soil spectroscopy have been published in Geoderma with 184 (Vis-NIR), 72 (MIR), and 46 (pXRF) papers; most of them were from the United States, China, Brazil, Australia, and India (Figure 2).

3.2 | Soil samples

The number of soil samples used in the prediction model using pXRF spectra mostly ranged from 50 to 200, whereas with Vis-NIR and MIR spectra, it mostly ranged from 51 to 300 (Figure 3). In general, the prediction model for soil properties using Vis-NIR and MIR spectra was used in a larger number of samples than pXRF spectra. Studies that had large numbers of soil samples (>600) were from Australia, Brazil, the United States, and several European countries. A few studies used less than 50 soil samples to perform the prediction model using Vis-NIR and MIR spectra; there are no studies that used less than 50 soil samples in the prediction model using pXRF spectra.

Most studies (82%) provided information on the sampling depth from which soil samples were taken. Some studies collected soil samples by horizon (O, A, B, A + B, or C), but most of them collected samples by fixed soil depths such as 0–20 cm and 20–40 cm. Studies focused on depths below 40 cm (Figure 3), sampled by soil horizon (A, B, and C), and investigated the relationship with soil color, parent material, lithologic discontinuity, or redoximorphic features. The deeper soil studies mainly used the pXRF.

Soil classification was not given in 21% of the papers. Some 20% of studies used only Australian (3%), Brazilian (<1%), Canadian (<1%), and Chinese (4%) classification systems or World Reference Base (11%). One-fifth of the studies did not include soil classification. Considering studying intensity, Entisols, Alfisols, and Inceptisols were mostly studied by pXRF spectrometer, whereas Vis-NIR and MIR spectrometers were often used for studying Alfisols, Inceptisols, and Entisols (Figure 3). A few studies focused on the prediction of soil physical and chemical properties of Gelisols.

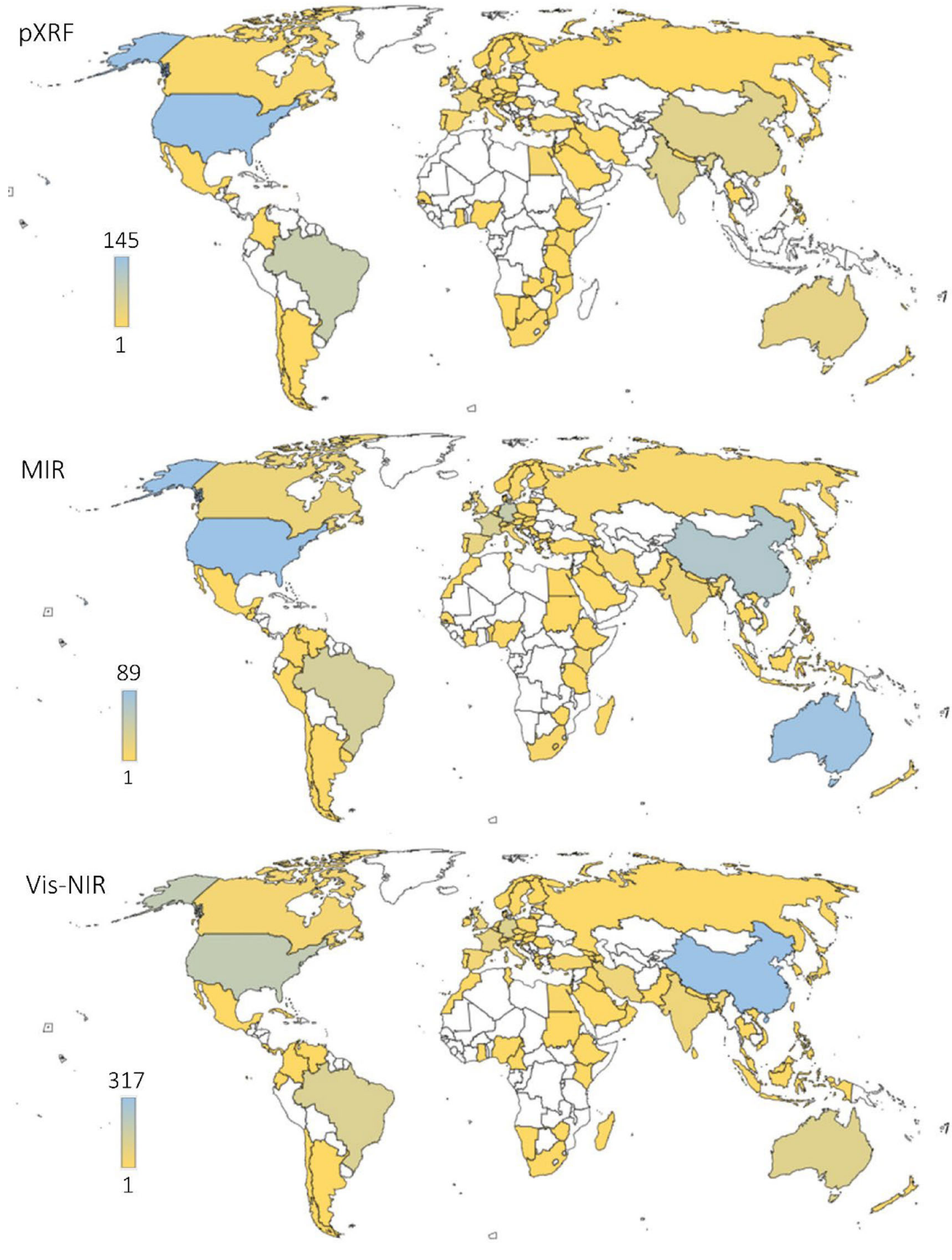

FIGURE 2 The number of papers for the characterization and prediction of soil properties considering the origin of the author(s) using portable X-ray fluorescence (pXRF) ($n = 301$), mid-infrared (MIR) ($n = 404$), and visible near-infrared (Vis-NIR) ($n = 1006$) spectra. Maps based on papers extracted from Scopus.

3.3 | Spectral range and prediction models

The used spectral range of Vis-NIR, MIR, and pXRF spectrometers for the prediction of soil properties is shown in Figure 4. About half of the papers used the visible region (350–750 nm) (40%) and MIR (2500–25,000 nm), whereas many of the papers (96%) used the full range of pXRF (0–50 keV) in the prediction models. More than half of the paper used limited soil spectra such as 400–2400 nm for Vis-NIR, 2500–17,000 nm for MIR, and 0–40 keV for pXRF. A decreasing trend in the spectral range was observed in the MIR region after 15,000 nm. The pXRF spectrometers are

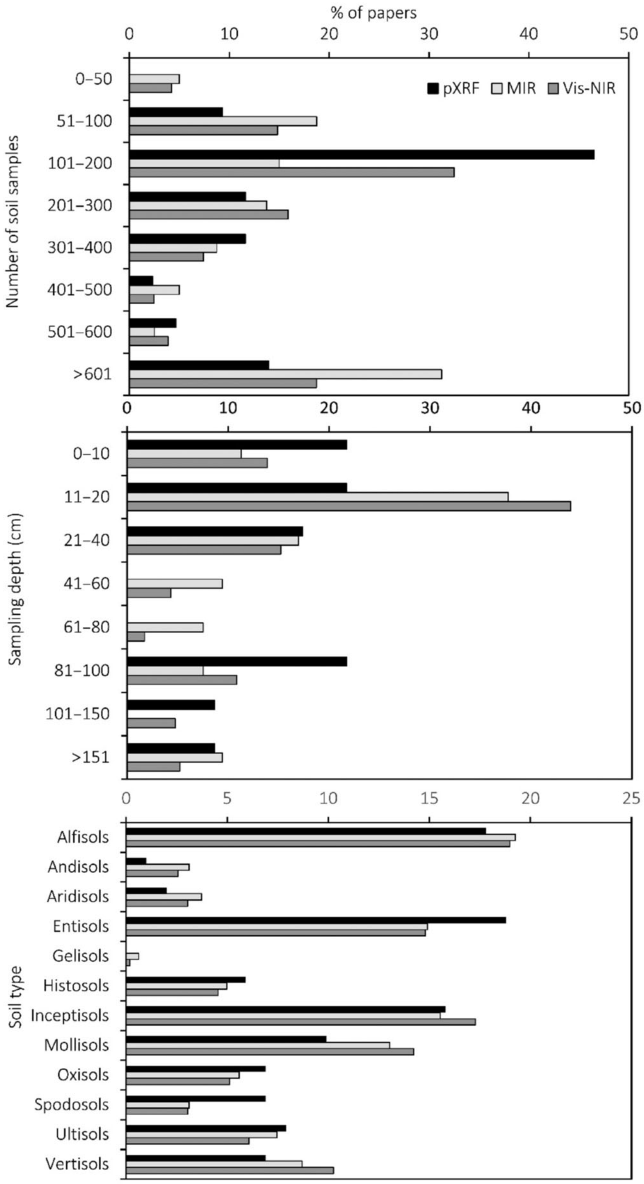

FIGURE 3 The number of soil samples, sampling depth, and soil type from 305 papers for each spectrometer (visible near-infrared [Vis-NIR], mid-infrared [MIR], and portable X-ray fluorescence [pXRF]).

mainly produced at energy levels of 0–35, 0–40, and 0–50 keV due to their operational capability. The exclusion of spectral noise ranges (i.e., 350–400, 350–450, and 350–500 nm) in the Vis-NIR spectral range were bigger than the MIR spectral range.

The partial least squares regression (PLSR) model was used in over half of the Vis-NIR and MIR studies (Figure 5) but its use is decreasing as it is replaced by random forests (RFs), cubist, support vector machine (SVM), support vector regression, and convolutional neural network (CNN) models. Half of the studies used RF, cubist, SVM, and PLSR models for the prediction of soil properties using a pXRF spectrometer. Almost 15% of papers used Bayesian model averaging, multivariate adaptive regression splines, generalized additive model, extreme gradient boosting, principal component regression, least absolute shrinkage and selection operator (Lasso), and elastic net (EN) models.

3.4 | Performance of model

The number of papers using pXRF, MIR, and Vis-NIR data for each soil property is given in Figure 6. Many studies focused on the prediction of SOC, clay, pH, and SOM when using Vis-NIR and MIR spectrometers; other studies focused on the prediction of pH and particle size distribution using pXRF data (Figure 6). For instance, SOC (135 and 51 papers), clay (83 and 32 papers), and pH (70 and 27 papers) were studied using Vis-NIR and MIR spectra, whereas clay (nine papers), pH (nine papers), sand (eight papers), silt (eight papers), TN (six papers), and TC (six papers) were studied by pXRF spectra. Few studies focused on $CaCO_3$ and SIC using Vis-NIR and MIR, and there were no papers studying SIC by pXRF spectra.

The mean and range in prediction accuracy (R^2) based on the validation results of using Vis-NIR, MIR, and pXRF spectra are shown in Figure 7 and Table 1. Most of the soil properties had better prediction metrics with MIR spectra. According to the mean value of the prediction accuracy (R^2) based on validation results for each soil property and spectrometer, MIR spectra had the best prediction accuracy with R^2 of 0.9 for SIC. MIR spectra had relatively lower prediction accuracy for silt, EC, and $CaCO_3$ when compared to Vis-NIR and pXRF spectra. The EC ($R^2 = 0.55$) was reasonably well predicted using Vis-NIR spectra, whereas silt ($R^2 = 0.63$) and $CaCO_3$ ($R^2 = 0.86$) were well predicted using pXRF spectra.

The highest prediction accuracy and some of its determining factors for each soil property and spectrometer (pXRF, MIR, and Vis-NIR) are given in Table 2. Vis-NIR and MIR spectra had the highest prediction accuracy with R^2 of 0.98 for sand, whereas pXRF spectra had an R^2 of 0.97 for silt.

3.5 | Prediction accuracy and year

The temporal trend of the highest prediction accuracies (R^2) for each spectrometer (pXRF, MIR, and Vis-NIR) is shown in Figure 8. There was an increasing trend in the prediction accuracy by year for sand, silt, clay, SIC, SOM, and EC when using MIR and Vis-NIR spectra. This increasing trend tended to be similar for TC and $CaCO_3$ when using pXRF spectra. This may be related to some factors: (i) advances in spectrometer technology, such as better resolution and calibration protocols; (ii) the use of advanced modeling techniques, including machine and deep learning; (iii) sampling strategies considering environmental variables, (iv) more

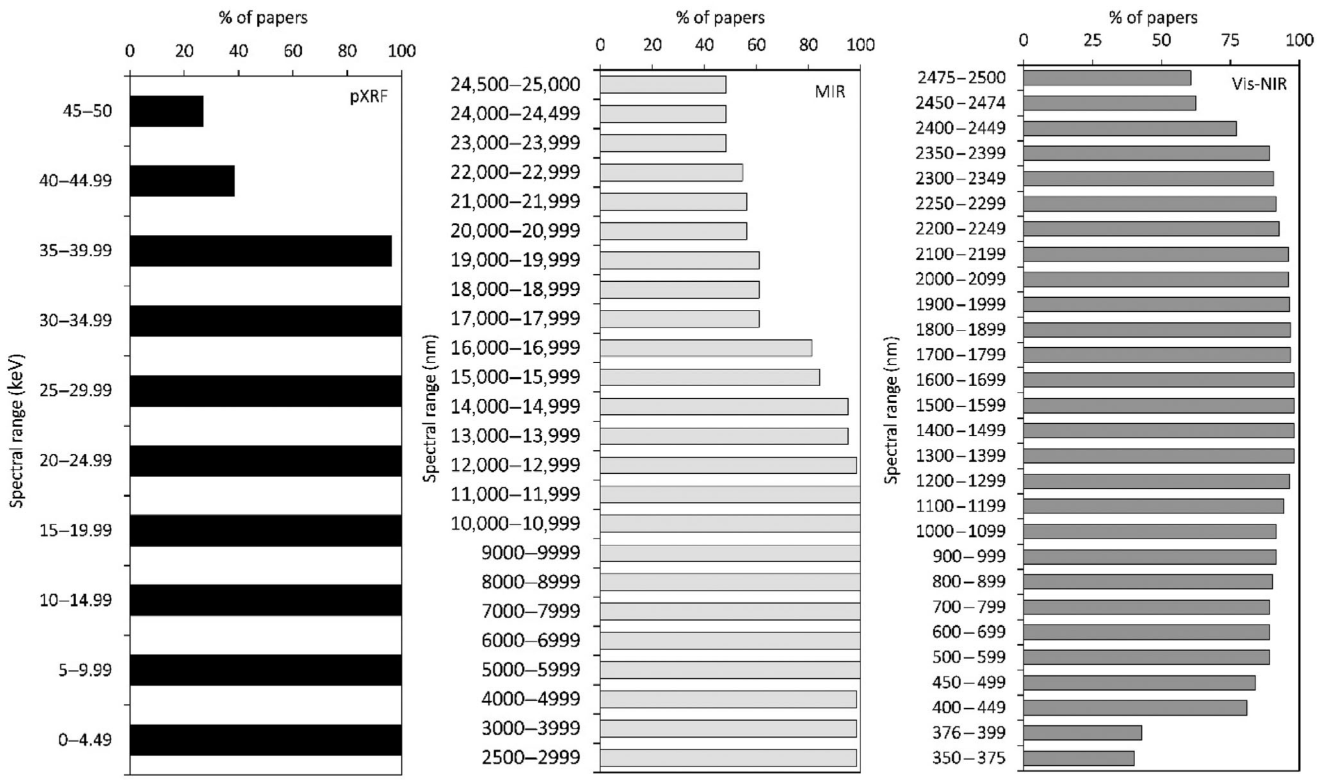

FIGURE 4 Spectral range based on portable X-ray fluorescence (pXRF; 0–50 keV), mid-infrared (MIR; 2500–25,000 nm), and visible near-infrared (Vis-NIR; 350–2500 nm) spectra for selected papers (n = 305). Each study used a different range of soil spectra (Vis-NIR, MIR, and pXRF) due to the preprocessing methods, the capability of the spectral range of the spectrometer, and the spectral preference of the study.

experience with spectrometers and data processing, leading to improved methods and more accurate results; and (v) optimized analytical protocols.

4 | DISCUSSION

There are several factors affecting the prediction accuracy for soil physical and chemical properties when using pXRF, MIR, and Vis-NIR spectra. These factors can be categorized as soil-based factors (i.e., parent material, soil mineralogy, soil type, and soil horizon/depth) and researcher-based factors (i.e., type or brand of spectrometer, which differ in hardware, spectral range, resolution, and calibration protocols, preprocessing methods, prediction models, and soil analysis methods for calibration). Few works have focused on the differences among the soil mineralogy, parent materials, and soil types to explore their impacts on the prediction accuracy of soil physical and chemical properties. This happens since they used classification models (e.g., decision tree, SVM, and RF) to predict soil mineralogy, soil parent materials, and soil type considering soil physical and chemical properties using pXRF, MIR, and Vis-NIR spectra (Acree et al., 2020; Andrade, Silva, Weindorf, Chakraborty et al., 2020; Gozukara et al., 2021; İnci et al., 2024; Mancini et al., 2019). They also reported that soil parent materials and soil types were mainly predicted by these spectrometers. Many studies have mainly focused on differences among horizon/depth, type or brand of spectrometer, which differ in hardware, spectral range, resolution, and calibration protocols, preprocessing methods, prediction model, and soil analysis methods for calibration to determine their impacts on the prediction accuracy of target soil properties. Therefore, we first reviewed researcher-based factors (i.e., type or brand of spectrometer, which differ in hardware, spectral range, resolution, and calibration protocols; preprocessing methods; prediction model; and soil analysis methods for calibration) and second reviewed soil-based factors (parent material, soil mineralogy, soil type, and soil horizon/depth).

4.1 | Researcher-based factors

4.1.1 | Different spectrometers

Different types of spectrometers have been used, all of which can vary in spectral ranges, resolutions, and optic sensors. The pXRF spectrometers vary at different spectral ranges such as 0–40 keV, 0–45 keV, and 0–50 keV (Table 2). One main difference between the studied sensors is that many of the pXRF equipment already comes, inside, with a black-box model to

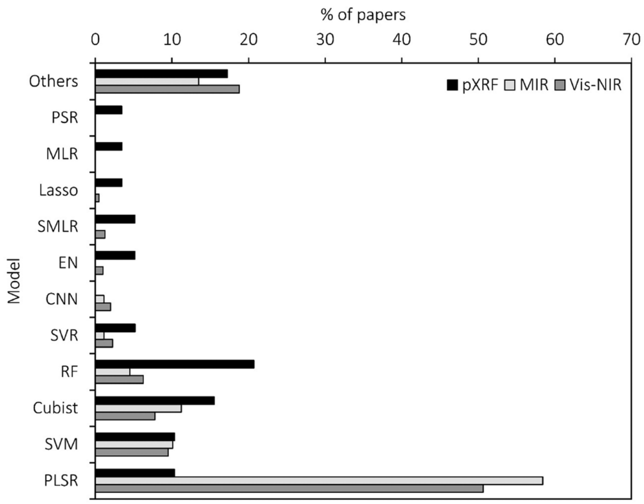

FIGURE 5 Type of models used for prediction of soil properties using visible near-infrared (Vis-NIR), mid-infrared (MIR), and portable X-ray fluorescence (pXRF) spectra based on 305 papers. The category "Others" contains Bayesian model averaging (BMA), wavelet neural networks (WNN), wavelet geographically weighted regression (WGWR), back propagation neural network (BPNN), local Gaussian regression (LGR), artificial neutral network (ANN), extreme learning machines (ELM), ordinary least square (OLS), multivariate adaptive regression splines (MARS), generalized additive model (GAM), extreme gradient boosting (XGBoost), boosted regression trees (BRT), gradient boosting decision tree (GBR), and principal component regression (PCR). CNN, convolutional neural network; EN, elastic net; Lasso, least absolute shrinkage and selection operator; MLR, multiple linear regression; PLSR, partial least squares regression; PSR, penalized-spline signal regression; SMLR, stepwise multiple linear regression; SVM, support vector machine; SVR, support vector regression.

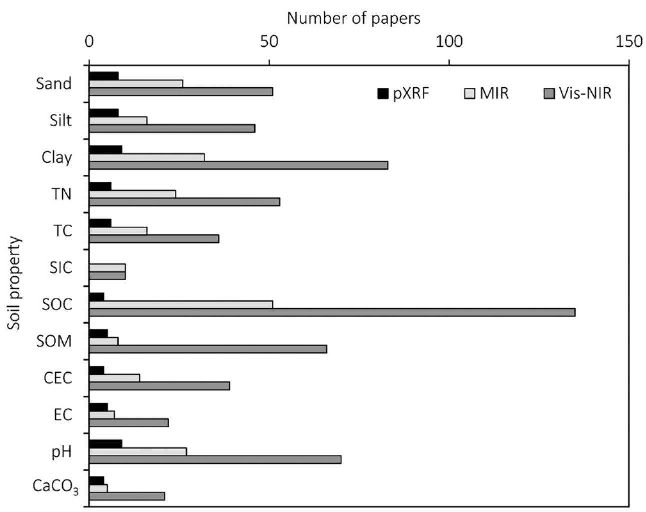

FIGURE 6 The number of papers using portable X-ray fluorescence (pXRF), mid-infrared (MIR), and visible near-infrared (Vis-NIR) spectra for each soil property. CEC, cation exchange capacity; EC, electrical conductivity; SIC, soil inorganic carbon; SOC, soil organic carbon; SOM, soil organic matter; TC, total carbon; TN, total nitrogen.

quantify the elements in the soil sample. With this information, the user directly compared the result of the sensor (result of the element) with the real wet soil analysis. The premise is that each element already has a specific band and peak. On the other hand, some studies create their own dataset to relate the spectra acquired from the equipment with the wet soil analysis. This black-box does not have, for instance, inside the Vis-NIR and MIR instruments. In this case, all papers depict the pure reflectance and have to create the dataset to finally relate with the wet soil analysis and then reach the model.

Many studies using Vis-NIR compared spectral ranges collected from several spectrometers such as Agrispec (350–2500 nm), Fieldspec (350–2500 nm), Terraspec (350–2500 nm), SM-3500 (350–2500 nm), NeoSpectra (1250–2500 nm), and NIRVascan (900–1700 nm). For example, Knadel et al. (2013) used five different spectral ranges based on different brands of spectrometers for the prediction of SOC and clay content. They found that spectral ranges had considerable influence on the prediction accuracy of SOC and clay with the R^2 ranging between 0.35 and 0.59 for SOC and 0.68 and 0.77 for clay. Tang et al. (2020) compared the prediction performance of four different portable infrared instruments for clay, sand, silt, pH, SOC, and CEC. They observed slight differences in the spectral pattern and the prediction accuracy of almost all soil properties. The spectral capability of spectrometers differs, and some have a limited spectral range (e.g., 1250–2500 nm and 900–1700 nm).

Vis-NIR spectra have different resolutions across the spectrum. In contrast, MIR and pXRF spectra maintain the same resolution across the full spectrum. However, the spectral resolution may vary depending on the brands of spectrometers. Gozukara, Acar et al. (2022) reported that the spectral resolution was 3 nm from 350 to 1000 and 10 nm from 1000 to 2500 nm in the prediction model when using Vis-NIR spectra. Zhang and Hartemink (2020) reported that the spectral resolution was 3, 8, and 6 nm for the spectral ranges of 350–1000 nm, 1000–1900 nm, and 1900–2500 nm in the prediction model with Vis-NIR spectra. Knadel et al. (2013) and Viscarra Rossel et al. (2016) reported that different resolutions of instruments did not greatly affect the prediction models. They also reported that the prediction accuracy might not be affected by the spectral range of spectrometers rather than the spectral resolution since it is possible to adjust the resolution of spectra by several techniques.

Other reasons for the heterogeneity in the spectra are the calibration protocols (e.g., type of reference material and calibration time before and after measurements), optical types of measuring equipment (e.g., contact probe, muglight, and fiber-optic probe under external halogen lamps), the size of the Petri dishes for measuring spots, the thickness of soils in the dish, repeated measurements per samples (and how to perform), the surface flatness of samples, and the particle size of soil samples (e.g., <2 mm for Vis-NIR and

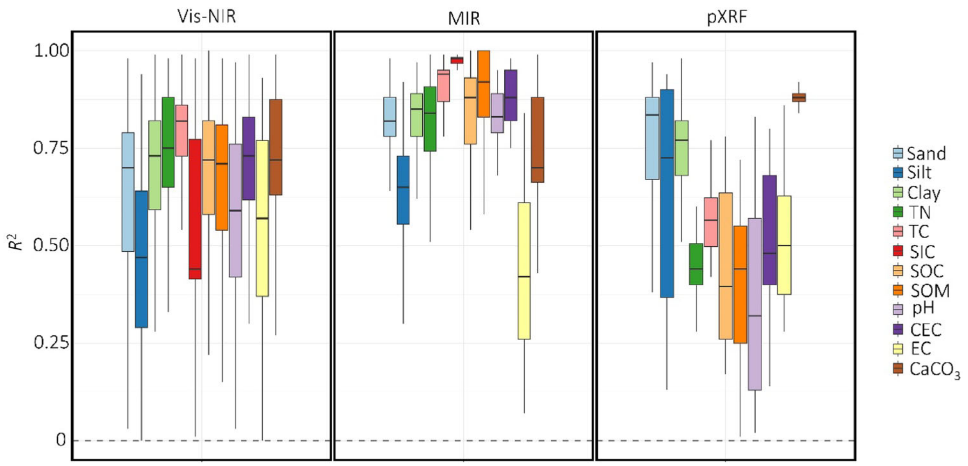

FIGURE 7 Predicting accuracy (R^2 values) extracted from 305 papers based on validation results for different soil physical and chemical properties using visible near-infrared (Vis-NIR), mid-infrared (MIR), and portable X-ray fluorescence (pXRF) spectra. Each box shows the minimum (lower line end), first quartile (Q1, lower box section), median (line within box), third quartile (Q3, upper box section), and maximum (upper line end). CEC, cation exchange capacity; EC, electrical conductivity; SIC, soil inorganic carbon; SOC, soil organic carbon; SOM, soil organic matter; TC, total carbon; TN, total nitrogen.

TABLE 1 Predicting accuracy (mean R^2 ± standard deviation) based on validation results for soil physical and chemical properties using Vis-NIR, MIR, and pXRF spectra (based on 305 studies).

	Vis-NIR	MIR	pXRF
Sand	0.62 ± 0.25b	0.82 ± 0.09a	0.74 ± 0.21a
Silt	0.46 ± 0.25b	0.60 ± 0.19a	0.63 ± 0.26a
Clay	0.69 ± 0.19b	0.83 ± 0.08a	0.73 ± 0.17b
Total nitrogen	0.73 ± 0.18b	0.79 ± 0.19a	0.44 ± 0.16c
Total carbon	0.78 ± 0.14b	0.90 ± 0.10a	0.58 ± 0.11c
Inorganic carbon	0.52 ± 0.28b	0.97 ± 0.04a	–
Organic carbon	0.68 ± 0.20b	0.82 ± 0.16a	0.44 ± 0.23c
Soil organic matter	0.66 ± 0.20b	0.87 ± 0.18a	0.38 ± 0.21c
Cation exchange capacity	0.69 ± 0.19b	0.89 ± 0.07a	0.50 ± 0.18c
Electrical conductivity	0.55 ± 0.24ns	0.44 ± 0.29ns	0.53 ± 0.19ns
pH	0.58 ± 0.22b	0.77 ± 0.23a	0.36 ± 0.23c
$CaCO_3$	0.71 ± 0.22b	0.73 ± 0.19ab	0.86 ± 0.11a

Note: Each soil property for Vis-NIR, MIR, and pXRF with different letters is significantly different at $p \leq 0.05$. ns, nonsignificant ($p > 0.05$).
Abbreviations: MIR, mid-infrared; pXRF, portable X-ray fluorescence; Vis-NIR, visible near-infrared.

pXRF and <0.15 mm for MIR spectrometers). Many studies used the polytetrafluoroethylene white reference (Spectralon) (Vis-NIR) (Demattê, Ramirez-Lopez et al., 2017; Zhang & Hartemink, 2021), anodized aluminum or a coarse gold-plated reference cap (MIR) (Hutengs et al., 2021; Ng et al., 2019), and a 316 stainless steel calibration check reference (pXRF) (Gozukara et al., 2021; Zhu et al., 2011) to calibrate the spectrometers. Recent papers on Vis-NIR and MIR spectrometers utilized calibration procedures after 10 (Greenberg et al., 2022; Seidel et al., 2022), 15 (Seidel et al., 2022), and 20 min (Dotto et al., 2017) of measurement time or after 10 (Gozukara, Acar et al., 2022; Stevenson et al., 2023) or 20 (Dotto et al., 2017) soil sample scanning with two or three main replications. There are some differences in the calibration procedures of Vis-NIR and MIR spectrometers. When combining datasets at regional, national, global, or continental scales, the spectral range of Vis-NIR, MIR, and pXRF spectrometers, as well as the resolution of spectra, cannot be controlled. Viscarra Rossel et al. (2016) suggested that if soil spectra were combined with other spectral data obtained by different research (e.g., regional or global), they should contain the same spectral range with 1, 2, 5, or 10 nm spectral resolution and be measured from air or oven-dry soil crushed or sieved using a 2-mm sieve.

TABLE 2 The highest prediction accuracy (R^2) based on validation results among selected papers ($n = 305$) for soil physical and chemical properties.

Property	Spectra	Spectral range (keV–nm)	Brand of spectrometer	Model of spectrometer	Preprocessing methods	Model	Method of analysis	Range of property	Number of soil samples	Depth (cm) or horizon	Soil order	R^2	Reference
Sand (%)	pXRF	0–40	Olympus	Innov-X Delta Premium	SG	Cubist	Bouyoucos	0.65–92	176	B	Alfisols, Mollisols	0.97	Gozukara, Zhang et al. (2022)
	MIR	2500–16,666	Bruker	TENSOR–27	COE, SLS, MSC, VN	PLSR	Bouyoucos	7–90	432	–	Oxisols	0.98	Cobo et al. (2010)
	Vis-NIR	400–2500	NIRSytems	6500	RS, SNVD, SNV, D	PLSR	Bouyoucos	2.7–72.4	150	20	Alfisols, Andisols, Aridisols, Entisols, Histosols, Inceptisols, Mollisols, Oxisols, Ultisols, Vertisols	0.98	Nduwamungu, Ziadi, Tremblay et al. (2009)
Silt (%)	pXRF	0–40	Olympus	Delta Premium	SG	Cubist	Bouyoucos	1.92–8.36	176	B	Alfisols, Mollisols	0.97	Gozukara, Zhang et al. (2022)
	MIR	–	Bruker	Vertex 70	BOT	MBL	Pipette	0–94.5	34,913	–	Alfisols, Andisols, Aridisols, Entisols, Gelisols Histosols, Inceptisols, Mollisols, Spodosols, Ultisols, Vertisols	0.92	Sanderman et al. (2020)
	Vis-NIR	400–2500	NIRSytems	6500	RS, SNVD, SNV, D	PLSR	Bouyoucos	16.3–41.4	150	20	Alfisols, Andisols, Aridisols, Entisols, Histosols, Inceptisols, Mollisols, Oxisols, Ultisols, Vertisols	0.93	Nduwamungu, Ziadi, Tremblay et al. (2009)
Clay (%)	pXRF	0–40	Olympus	Innov-X Delta Premium	–	BSWMLR	Pipette	3.70–40	426	40	Alfisols, Entisols, Inceptisols, Mollisols Vertisols	0.98	Zhu et al. (2011)
	MIR	2500–16,666	Bruker	Vertex 70	BOT	MBL		–	33,156	–	Alfisols, Entisols, Inceptisols	0.97	Dangal et al. (2019)
	Vis-NIR	400–2500	NIRSytems	6500	RS, SNVD, SNV, D	PLSR	Bouyoucos	27.4–58.6	150	20	Alfisols, Andisols, Aridisols, Entisols, Histosols, Inceptisols, Mollisols, Oxisols, Ultisols, Vertisols	0.99	Nduwamungu, Ziadi, Tremblay et al. (2009)

(Continues)

TABLE 2 (Continued)

Property	Spectra	Spectral range (keV–nm)	Brand of spectrometer	Model of spectrometer	Preprocessing methods	Model	Method of analysis	Range of property	Number of soil samples	Depth (cm) or horizon	Soil order	R^2	Reference
TN (%)	pXRF	0–45	Olympus	DP-600 Delta	–	RF	Dumas Com	0–0.01	675	40	Alfisols, Entisols, Mollisols	0.90	D. Wang et al. (2015)
	MIR	2500–25,000	Bruker	Vertex 70	ATR Cor.	Cubist	Dry combustion	0–3.3	700	100	Alfisols, Andisols, Aridisols, Entisols, Histosols, Inceptisols, Mollisols, Oxisols, Ultisols, Vertisols	0.99	Haghi et al. (2021)
	Vis-NIR	350–2500	Oceon Optics	QE-65000	SG, MSC, FT	PLSR	Dry combustion	0.06–0.16	44	30	Mollisols, Alfisols	0.98	J. Liu et al. (2020)
TC (%)	pXRF	0–40	Olympus	Innov-X Delta Premium	SG	Cubist	Dry combustion	0–9.9	324	A + B	Alfisols, Mollisols	0.87	Gozukara, Zhang et al. (2022)
	MIR	2500–25,000	Bruker	Vertex 70	ATR Cor.	Cubist	Dry combustion	0.02–57.05	700	100	Alfisols, Andisols, Aridisols, Entisols, Histosols, Inceptisols, Mollisols, Oxisols, Ultisols, Vertisols	0.99	Haghi et al. (2021)
	Vis-NIR	1100–2500	FOSS NIRSystems	5000	ATR Cor.	CNN	Dry combustion	0.02–57.05	700	100	Alfisols, Andisols, Aridisols, Entisols, Histosols, Inceptisols, Mollisols, Oxisols, Ultisols, Vertisols	0.99	Haghi et al. (2021)
SIC (%)	pXRF	–				–		–		–	–	–	–
	MIR	2500–16,666	Bruker	Vertex 70	–	ANN	HCL treatment	0–12.62	20,153	–	Mollisols	0.99	Wijewardane et al. (2018)
		2500–25,000	Thermo Fischer	Nicolet 6700	SNV, D, SNVD, MSC,	PLSR	–	0–10.4	2178	50	–	0.99	Barthès et al. (2020)
		2500–15,385	Agilent	4300	MSC, SNV, L1-NV	PLSR	Dry combustion	0.55–3.99	80	15	Alfisols, Entisols, Inceptisols, Mollisols, Vertisols	0.99	Hutengs et al. (2021)
	Vis-NIR	400–2498	FOSS NIRSystems	6500	RS	PSLR	Dry combustion	0–2.56	311	30	Mollisols	0.98	Chang et al. (2005)
		400–2500	ASD	FieldSpec 3	MSC, SNV, L1-NV	PLSR	Dry combustion	0.55–3.99	80	15	Alfisols, Entisols, Inceptisols, Mollisols, Vertisols	0.99	Hutengs et al. (2021)

(Continues)

TABLE 2 (Continued)

Property	Spectra	Spectral range (keV–nm)	Brand of spectrometer	Model of spectrometer	Preprocessing methods	Model	Method of analysis	Range of property	Number of soil samples	Depth (cm) or horizon	Soil order	R^2	Reference
SOC (%)	pXRF	0–40	Olympus	Innov-X Delta	–	Cubist	Walkey-Black	9.9–98	158	25	–	0.78	John et al. (2021)
	MIR	2500–16,666	Bruker	Vertex 70	BOT	MBL	Dry combustion	–	33,156	–	Alfisols, Entisols, Inceptisols	1.00	Dangal et al. (2019)
		–	Bruker	Vertex 70	BOT	MBL	TC-carbonates	0–65.6	53,673	–	Alfisols, Andisols, Aridisols, Entisols, Gelisols, Histosols, Inceptisols, Mollisols, Spodosols, Ultisols, Vertisols	1.00	Sanderman et al. (2020)
	Vis-NIR	350–2500	ASD	Labspec	RS	PLSR	Dry combustion	0–65.5	19,891	–	–	0.98	Wijewardane et al. (2016)
SOM (%)	pXRF	0–50	Bruker	S1 Titan LE	–	RF	Walkey–Black	0.04–18.21	705	100	Entisols, Inceptisols, Histosols, Oxisols, Ultisols	0.64	de Faria et al. (2022)
	MIR	2500–16,666	Bruker	INVENIO	RS, MSC, SVN, EMSC	Cubist	LOI	2.6–7.4	9503	115	Alfisols, Entisols, Inceptisols, Histosols, Spadosols, Ultisols	1.00	de Santana et al. (2022)
	Vis-NIR	350–2500	ASD	FieldSpec 4	SG, SNV, MSC, NOR	PLSR	Combustion	1.18–2.69	44	30	Mollisols, Alfisols	0.98	J. Liu et al. (2020)
Property	**Spectra**	**Spectral range (keV–nm)**	**Brand of spectrometer**	**Model of spectrometer**	**Preprocessing methods**	**Model**	**Method of analysis**	**Range**	**Number of soil samples**	**Depth (cm) or horizon**	**Soil order**	**R^2**	**Reference**
CEC (cmol kg^{-1})	pXRF	0–35	Bruker	Tracer III-SD	–	MPLSR	–	–	102	20	Alfisols, Andisols, Aridisols, Entisols, Histosols, Inceptisols, Mollisols, Oxisols, Ultisols, Vertisols	0.80	Tavares et al. (2020)
	MIR	2500–16,666	Bruker	Vertex 70	BOT	MBL	–	–	33,156	–	Alfisols, Entisols, Inceptisols	0.99	Dangal et al. (2019)
	Vis-NIR	350–2500	ASD	FieldSpec 3	RS, CT	Cubist	–	0–958	17,433	–	Alfisols, Entisols, Inceptisols	0.99	Demattê et al. (2019b)

(Continues)

TABLE 2 (Continued)

Property	Spectra	Spectral range (keV–nm)	Brand of spectrometer	Model of spectrometer	Preprocessing methods	Model	Method of analysis	Range	Number of soil samples	Depth (cm) or horizon	Soil order	R^2	Reference
EC (dS m^{-1})	pXRF	0–40	ASD	FieldSpec 3	RS, SG, MSC, SNV, D, CR	PLSR	Saturated paste	1.45–73.9	130	30	Aridisols, Entisols	0.84	Naimi et al. (2022)
	MIR	–	Bruker	Vertex 70	BOT	MBL	Saturated paste	0–25	614	–	Alfisols, Andisols, Aridisols, Entisols, Gelisols, Histosols, Inceptisols, Mollisols, Spodosols, Ultisols, Vertisols	0.84	Sanderman et al. (2020)
	Vis-NIR	500–2450	ASD	FieldSpec 4	RS, SG, SNV	SVM	1:1, 1:2.5 (soil:water)	0.01–8.37	100	100	Alfisols	0.93	Gozukara, Altunbas et al. (2022)
pH	pXRF	0–40	Olympus	Innov-X Delta Premium	–	MLR	1:1, (soil:water)	4.17–8.61	639	–	Alfisols, Entisols, Inceptisols, Mollisols, Spodosols, Ultisols, Vertisols	0.77	Sharma et al. (2014)
	MIR	2500–16,666	Bruker	Vertex 70	RS, SG, SNV	Cubist	soil:water	2.86–10.32	14,594	–	–	0.94	Ng et al. (2019)
	Vis-NIR	350–2500	ASD	FieldSpec 3	CT	PLSR		0–8.9	17,433	120	Alfisols, Entisols, Inceptisols, Mollisols, Vertisols	0.97	Demattê et al. (2019b)
$CaCO_3$ (%)	pXRF	0–40	Olympus	Vanta M	–	BRT	Calcimetry	1.81–34.45	300	120	Alfisols, Entisols, Inceptisols, Histosols, Spodosols, Ultisols	0.92	Acree et al. (2020)
	MIR	2500–16,666	Bruker	Vertex 70	RS	PLSR	Equivalent	–	594	–	Mollisols	0.99	Seybold et al. (2019)
	Vis-NIR	450–2500	ASD	LapSpec 5000	RS, D, SNV, MSC, IMSC, WMSC	MPLSR	Calcimetry	0–85	201	20	Alfisols, Inceptisol, Vertisols	0.99	Gras et al. (2014)

Abbreviations: ANN, artificial neutral network; ATR Cor., attenuated total reflectance correction; BOT, baseline-offset correction; BRT, boosted regression trees; BSWMLR, backward step-wise multiple linear regression; CEC, cation exchange capacity; CNN, convolutional neural network; COE, constant offset elimination; CR, continuum removal transformation; CT, continuum removal; D, detrending; EC, electrical conductivity; EMSC, extended multiplicative signal correction; FT, Fourier transform; HCl, hydrochloric acid; IMSC, inverse LOI, loss on ignition; MBL, memory-based learning; MIR, mid-infrared; MPLSR, modify partial least squares regression; MSC, multiplicative scatter correction; MSC; L1-NV, L1-norm vector normalization; NOR, normalization, PLSR, partial least squares regression; pXRF, portable X-ray fluorescence; RF, random forest; RS, spectral range selection (reducing); SG, Savitzky–Golay filtering; SIC, soil inorganic carbon; SLS, straight line subtraction; SNV, standard normal variate; SNVD, standard normal variate transformation detrending; SOC, soil organic carbon; SOM, soil organic matter; SVM, support vector machine; TC, total carbon; TN, total nitrogen; Vis-NIR, visible near-infrared; VN, vector normalization; WMSC, weighted MSC.

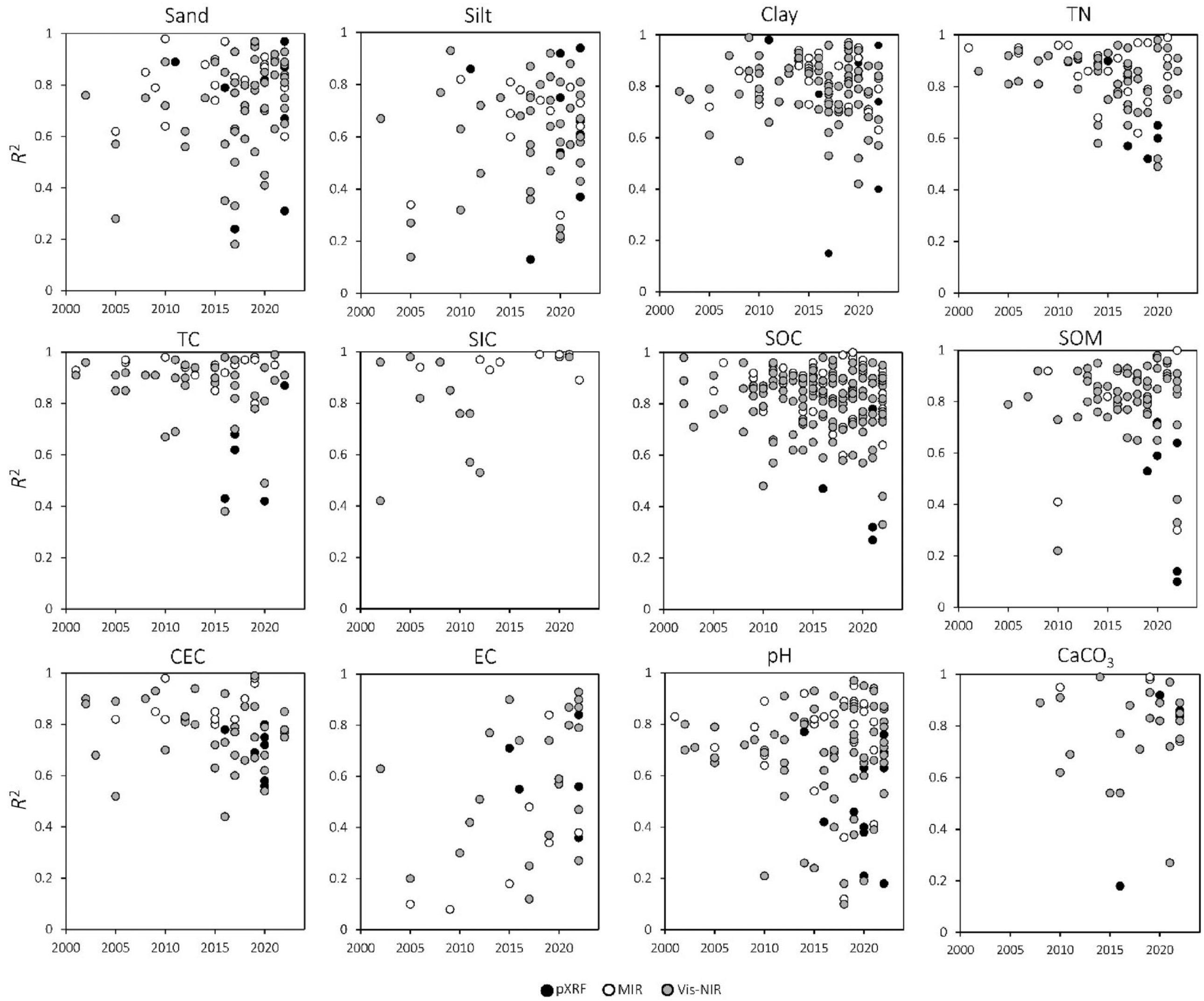

FIGURE 8 The relationship between the highest R^2, which was obtained from 305 papers, over time for each spectrometer (portable X-ray fluorescence [pXRF], mid-infrared [MIR], and visible near-infrared [Vis-NIR]) and soil property. CEC, cation exchange capacity; EC, electrical conductivity; SIC, soil inorganic carbon; SOC, soil organic carbon; SOM, soil organic matter; TC, total carbon; TN, total nitrogen.

4.1.2 | Preprocessing methods

Preprocessing methods have been applied to remove noise because of light scattering, transform spectral data, and accentuate features for prediction or characterization modeling. In multivariate calibration, preprocessing processes of soil spectra are critical (Stark, 1988) and improve the prediction accuracy (Dunn et al., 2002; Shi et al., 2023; Vasques et al., 2008; Zhang & Hartemink, 2020). The selection of ranges due to spectral noise, smoothing, feature selection, normalization, baseline correction, scatter correction, and derivates has been commonly used as preprocessing methods for soil spectroscopy (Dotto et al., 2017, 2018; Nawar et al., 2016; Shi et al., 2023; Vasques et al., 2008; Zhang & Hartemink, 2020). Preprocessing methods can be divided into two groups: scatter correction and spectral derivates (Rinnan et al., 2009). Scatter correction includes normalization by range, continuum removal, multiplicative scatter correction, and standard normal variates, whereas spectral derivatives are represented by Savitzky–Golay (SG) and Norris–Williams derivatives.

Spectral noise can arise from various sources such as signal interference, signal distortion, quantization error, impulsive noise, thermal noise, and the surface of samples can impact the quality and clarity of a signal (Hayes, 1996; Proakis & Manolakis, 2006). Studies have generally removed some parts, including such as 350–400 nm (Tian et al., 2013), 350–450 nm (Kuang & Mouazen, 2012), 350–500 nm (Sun et al., 2018; J. Wang et al., 2014), and 2450–2500 nm (Gozukara, Acar et al., 2022; J. Wang et al., 2014) in the Vis-NIR region and 2500–2505 nm (Viscarra Rossel & Lark, 2009), 2500–2564 nm (Mirzaeitalarposht & Kambouzia, 2020), and 2500–2600 nm (Hong, Munnaf et al., 2022) in the MIR region. A wider range from Vis-NIR spectra is generally removed compared to MIR spectra, which can be attributed to the stability of the MIR spectral region. Several studies preferred the full range of Vis-NIR (350–2500 nm) (Di lorio et al., 2022; Leue et al., 2019; Lucà et al., 2017) and MIR (2500–25,000 nm) (Barthès et al., 2020; Chevallier et al., 2019). The lack of removing noise in the spectra may be one of the reasons for the variation in prediction accuracy, since it creates an erratic information that has impacts on results.

The effect of preprocessing methods on the prediction performance differs between soil properties. Ben-Dor et al. (1997) focused on the effects of the first and second derivatives of Vis-NIR spectra for the characterization of SOM. Spectral derivation contributed to enhancing spectral features and characterization of SOC. Vasques et al. (2008) compared several preprocessing methods, such as Norris–Williams and SG derivates, reflectance-to-absorbance and Kubelka–Munk transformation, baseline offset, normalization, and standardizations to achieve relatively higher prediction accuracy using Vis-NIR spectra. They noted that SG derivates had better accuracy in the prediction of SOC. Similarly, Nawar et al. (2016) achieved the highest prediction accuracy with the continuum-removed reflectance preprocessing method using Vis-NIR spectra for clay and SOM when comparing seven different preprocessing methods. These seven preprocessing methods were applied to the raw spectral Vis-NIR spectral signature for SOC to improve the prediction accuracy by Dotto et al. (2018). They reported that there were significant differences between the prediction accuracy and the best fit, with the highest prediction accuracy for SOC obtained by applying the normalization by range method. Similarly, the baseline offset correction (BOC), SG smoothing with first derivative, and spectral space transformation (SST) on MIR spectra to explore the effects of their performance in the prediction of TC, pH, and clay by Sanderman et al. (2023). They observed that BOC was the best method for the prediction of TC, pH, and clay than SG and SST preprocessing methods.

Many studies have used different preprocessing methods for pXRF spectra (e.g., Nawar et al., 2016; O'Rourke, Stockmann et al., 2016) but few studies compared the efficiency of preprocessing methods, such as Zhang and Hartemink (2020) who compared different preprocessing methods based on smoothing, including (i) Fourier transformation, (ii) moving average, (iii) Savitsky and Golay polynomial filter, and (iv) Gaussian filter, and background removal and peak search using pXRF spectra for prediction of sand, silt, clay, TC, TN, and pH. The preprocessing methods had different effects on different soil properties. The Savitzky and Golay polynomial filter and the Gaussian filter smoothing methods had better prediction accuracy compared to other methods. Similarly, Shi et al. (2023) evaluated the performance of baseline correction, scatter correction, and SG preprocessing methods for the prediction of SOM using pXRF spectra. They suggested that 1.6th-order derivative and baseline correction methods to achieve relatively higher prediction accuracy in the prediction of SOM.

4.1.3 | Prediction models

Investigating the complex nonlinear relationship between soil properties and soil spectra can be accomplished by machine learning models (Chen et al., 2022). Models such as SVM, RF, cubist, PLSR, lasso, EN, and ridge have been used, and in the last two decades, there has been an increasing trend in using deep learning models, including CNN based on one- or two-dimensional (Haghi et al., 2021; Hong, Chen et al., 2022; Li et al., 2020; Ng et al., 2019; Padarian et al., 2019; Tsimpouris et al., 2021), recurrent neural network using Vis-NIR, MIR, and pXRF spectra in soil science. Padarian et al. (2019) and Ng et al. (2019) used deep learning models, including CNN, which had a higher prediction accuracy in the prediction of TC, SOC, CEC, clay, sand, and pH compared to traditional machine learning models, including PLSR and cubist. The CNN model achieved higher prediction accuracy than cubist and PLSR models for each soil property. While each spectral range was traditionally used separately, the fusion of more than one range data has been performed by Terra et al. (2019). Using the outer product analysis system, they optimize carbon quantification by merging Vis-NIR with MIR. The deep learning models have relatively better prediction accuracy than machine learning models, although there are only a few studies, such as those of Padarian et al. (2019) and Ng et al. (2019). As reported by Demattê, Horak-Terra et al. (2017) and Gómez et al. (2022), it is important to understand the pedological information of soils before creating the populations to go forward on quantification. Indeed, more focus should be given on exploring the integration of pedological knowledge in the prediction models and exploring the efficiency of deep learning models using Vis-NIR, MIR, and pXRF spectra. In addition, it is important to mention that efforts should also be addressed to insert soil knowledge into machine-learning prediction of soil properties. This was first indicated by Marques et al. (2019). As concluded by Ma et al. (2023), statistical mechanisms can lead to inadequate conclusions or errors, which may be avoided by a soil expert on its interpretation. To help on this task, Demattê et al. (2014) developed the morphological interpretation of reflectance spectrum, where the soil expert can identify the soil properties before going to the statistics. This went further in three sequence papers to express the method of qualitative analysis of spectra for Vis-NIR, MIR (Silvero et al., 2020), and XRF (Rosin et al., 2022).

4.1.4 | Methods for soil analysis

Incorrect and mismatched soil spectra with laboratory data are a major problem in the prediction of soil properties

(Soriano-Disla et al., 2014). Standard analytical methods are essential to obtain reliable calibration (van Leeuwen et al., 2024), and wet soil analysis method has measurement errors and variations (Paiva et al., 2022). The problem increases when combining datasets that have different analytical methods (Reeves et al., 2010). For SOC analysis, Walkey and Black, dry or wet combustion, and potassium dichromate titration, or phosphorous (with resin or Mehlich) methods give different results (Conyers et al., 2011). Some other examples of differences between results and analytical methods are charcoal-C (Hammes et al., 2007), pH (Davies, 1971; Gozukara, Altunbas et al., 2022; Sonmez et al., 2008), and EC (Gozukara, Altunbas et al., 2022). Indeed, Demattê et al. (2019b) prepared a comparison of soil analysis between four wet laboratories and four spectrometers, all within the same soil sample. The conclusion was that the wet laboratories presented a greater difference between analyses, and this impacted spectral statistics. The sensors presented a lower variation between them. At the end, the better the quality of a laboratory soil analysis, the higher the quantification.

Stevenson et al. (2023) used Vis-NIR and MIR spectra to explore the effect of pipette and hydrometer methods on the prediction accuracy of sand content. Using MIR spectra, they obtained a relatively higher R^2 of 0.94 and 0.92 for the pipette and hydrometer methods, respectively; in contrast, with Vis-NIR spectra, they obtained R^2 of 0.93 and 0.91. Gozukara, Zhang et al. (2022) used Vis-NIR and pXRF spectra to compare the effect of soil:water ratios (1:1, 1:2.5, and 1:5) on the prediction accuracy of EC and pH. They obtained a relatively higher R^2 of 0.93 for EC and 0.81 for pH using Vis-NIR spectra with a 1:2.5 soil:water ratio derived from soil surface and profile, respectively. They also reported that Vis-NIR spectra had relatively higher prediction accuracy than pXRF spectra.

4.2 | Soil-based factors

4.2.1 | Parent material

Soil parent material influences the physical, chemical, and mineralogical properties of soils (Jenny, 1941). Lithologic discontinuity is challenging to identify in the field because they lack distinct morphological and physical expression (Price et al., 1975; Soil Survey Staff, 2014). Stable elements such as Ti and Zr have been used to explore soil uniformity in pedon (Hu et al., 2023) and lithologic discontinuity (Curi & Franzmeier, 1987; Gozukara et al., 2021; Grauer-Gray & Hartemink, 2018; Weindorf et al., 2015). Mancini et al. (2019) reported that V, Ni, Sr, and Pb can be successfully used for the prediction of the parent material. Gozukara et al. (2021) found the Ruxton index (SiO_2/Al_2O_3), Ti/Zr, and CaO/TiO_2 ratios to be robust indicators to distinguish terra rossa covered by loess. Mancini et al. (2020) found that soils developed from quartz and sandy sediments had relatively higher SiO_2 concentrations, whereas gabbro and basalt showed relatively lower SiO_2 concentrations. They also reported that Rb is robust to separate soils derived from quartzite, phyllite, and sandstone. Araujo et al. (2014) and S. H. G. Silva et al. (2020) distinguished soils from gneiss and gabbro based on a relatively high concentration of Ni and a relatively low concentration of Fe. Mendes et al. (2021) developed a framework to analyze soil mineralogy, which, in turn, could indicate the underlying geology. F. A. Mello et al. (2021) demonstrated the transition from laboratory to satellite spectra, highlighting the importance of spectroscopy in visualizing the spatial distribution of parent materials. Araujo et al. (2014) found that although the soils were derived from the same parent material, such as sandstone, the concentrations of As and Pb varied across soils, as geological formations can significantly influence these concentrations.

Vis-NIR and pXRF spectra can be used to distinguish and predict soil parent materials with high prediction accuracy (Gozukara et al., 2021; Mancini et al., 2019, 2023). Gozukara et al. (2021) compared the performance of Vis-NIR and pXRF spectra in predicting physicochemical properties and distinguishing parent materials. The pXRF spectra had better prediction accuracy compared to Vis-NIR spectra. Similarly, Weindorf et al. (2015) found that pXRF had better characterization performance for lithological discontinuity among loess, alluvium, lacustrine, marine, and aeolian sediments. This is related to differences in the elemental concentrations such as Ti, Zr, Si, and Al among parent materials. MIR spectra have not been used to distinguish the parent materials. When a soil contains high levels of particular elements, it may overshadow or mask other soil features in spectroscopic measurements. O'Rourke, Minasny et al. (2016) found that high concentrations of trace elements (e.g., Cd, As, and Mn) and heavy metals overshadowed spectral features associated with SOC and pH, making it difficult to isolate their signals when using Vis-NIR and pXRF spectra. They also reported that high Fe_2O_3 content, including basalt and mafic igneous rocks, ironstone or ferricrete, and laterites, strongly absorbs in Vis-NIR and MIR regions, masking signals from SOC and clay content, reducing prediction accuracy. Some parent materials, such as loess, alluvial deposits, sandstone, glacial outwash, eolian sands, and volcanic ash, generally contain high amounts of sand and silt. The high sand and silt content can mask the presence of clay, leading to low prediction accuracy for clay content (Zhang & Hartemink, 2020).

4.2.2 | Soil mineralogy

Few studies focused on the prediction of minerals, including gibbsite, goethite, hematite, kaolinite, muscovite, and quartz, using pXRF, MIR, and Vis-NIR spectra (Ma et al., 2024;

Rosin et al., 2023; Silvero et al., 2020). Kaolinite ($R^2 = 0.73$), hematite + goethite ($R^2 = 0.85$), muscovite + kaolinite ($R^2 = 0.73$ and 0.80), and muscovite ($R^2 = 0.81$) can be accurately predicted using individual or combined Vis-NIR and pXRF spectroscopy. Ma et al. (2024) reported that soil mineralogical compositions, including quartz ($R^2 = 0.76$–0.79), allophane/imogolite ($R^2 = 0.75$–0.81), gibbsite ($R^2 = 0.80$–0.85), mica ($R^2 = 0.81$–0.83), smectite ($R^2 = 0.62$–0.73), and kaolin-smectite ($R^2 = 0.72$–0.84), were well predicted using MIR spectra. Smectite, a 2:1 layer silicate, has broad and unclear OH stretching bands in the range of 3620–3630 cm^{-1}. These bands often overlap with those of kaolinite, water, amorphous silica, and other clay minerals. It has similar O–Si–O and O–Al–O stretching and deformation bands to other silicate minerals in the ranges of 1030–1020 cm^{-1} and 470–450 cm^{-1}. These overlapping bands make it harder to analyze and measure smectite. Rosin et al. (2023), Mendes et al. (2021), Silvero et al. (2020), and Poppiel et al. (2020) emphasized the significance of using spectra to analyze and measure soil minerals. The low prediction accuracy of quartz might be affected by the intensity of weathering and the loss of silica. The availability of Al facilitates the substitution of Fe, which occurs to a greater extent in goethite than in hematite; this substitution is more prominent under intense weathering conditions (Bigham et al., 2002; Fitzpatrick & Schwertmann, 1982). Aluminum affects the intensity and position of the peak corresponding to goethite in the spectral curves (Jiang et al., 2014). The EC, sand, clay, and SOC can be explained by the presence of soil minerals identified by peaks in the MIR and Vis-NIR spectra. The prediction of soil properties may be affected by the suppression and interference of minerals that differ in predominance or degree of weathering. For example, Scheinost et al. (1998) reported that the prediction of goethite was affected by the overlapping effect of secondary hematite wavelengths. SOM can also be masked by the high presence of iron oxides (hematite and goethite) and clay mineralogy in soil (Nduwamungu, Ziadi, Parent et al., 2009). Naimi et al. (2022) reported that the absorption peak at 2338 nm related to the presence of carbonate in the Vis-NIR region was masked due to the higher content of gypsum.

4.2.3 | Soil type

There is a need for nondestructive, cost-effective, and environmentally friendly technology for the classification of soils (Benedet et al., 2020). Proximal soil sensors, including Vis-NIR, MIR, and pXRF spectra, can be used for the characterization and prediction of soil classification (Acree et al., 2020; Andrade, Silva, Weindorf, Chakraborty et al., 2020; Vasques et al., 2014; Xie & Li, 2018) as there is a correlation between soil spectroscopy and physical, chemical, and mineralogical properties (Benedet et al., 2022; Gozukara, Altunbas et al., 2022). Acree et al. (2020) used Vis-NIR and pXRF spectrometers to classify 25 soil cores across five toposequences. Andrade, Silva, Weindorf, Chakraborty et al. (2020) used pXRF data to classify 734 soil samples into five different soil orders (Ultisols, Incepstisols, Entisols, Oxisols, and Histosols). Xu et al. (2020) used Vis-NIR and MIR spectra to classify 146 soil profiles into eight soil orders. They reported that MIR spectra had relatively higher accuracy in classifying soil orders compared to Vis-NIR spectra. Gómez et al. (2022) and Greschuk et al. (2023) made two Brazilian states complete spectral characterization and quantification and indicated distinct methodological approaches to reach soil classification by proximal Vis-NIR spectra. Demattê, Horak-Terra et al. (2017) were able to relate wetland soil types with Vis-NIR as well.

Benedet et al. (2020) utilized Vis-NIR and pXRF spectra to classify 11 soil subgroups from Ultisols, Inceptisols, Spodosols, Oxisols, and Entisols. They focused on the effect of soil horizons, including individual A and B horizons and combined A + B horizons, on the prediction of soil suborders. Higher prediction accuracy was obtained using pXRF spectra in B horizons compared to individual A and combined A + B horizons.

Zhang et al. (2021) used MIR spectra to classify 270 soil profiles into eight soil orders with five master horizons (O, A, E, B, and C) and five B horizons (Bhs, Bs, Bk, Bt, and Bw). The MIR spectra could be used to classify soil orders, master, and B horizons. Zhang et al. (2021) and Weerasekara et al. (2024) found that Histosols and Spodosols had similar absorption features in their organic-rich O horizons, but their subsoils (E, Bhs, and Bs) differed. These differences made Spodosols easily distinguishable from other soil orders. Çullu et al. (2024) reported that Inceptisols, Entisols, and Vertisols had different spectral patterns due to their characteristic Ap, Ad, Bk, Bw, and Ck horizons for their characterization. Soils with more sand, like Aridisols, Spodosols, and Entisols, showed weaker absorption at 3695 and 3620 cm^{-1} (O–H bonds in clay minerals) and 916 cm^{-1} (Al–OH in clay minerals) compared to clay-rich soils like Alfisols and Mollisols. Carbonate peaks around 2517 cm^{-1} were prominent in soils with high $CaCO_3$, such as Entisols, Inceptisols, and some Aridisols and Mollisols. However, Mollisols, Ultisols, Aridisols, and Inceptisols had similar MIR spectra, making them harder to distinguish. The spectral characteristics of soil orders were strongly linked to their horizons and the related soil properties (Zhang et al., 2021). For instance, Andisols, with their high allophane content, show a smooth spectral pattern from 3700 to 3000 nm^{-1}. These soils are easier to predict compared to granular, oxidic, and ultic soils, which are typically older and more developed, with an average clay content of 47%–62% and dominated by kaolin minerals, showing strong kaolinite bands. However, when the clay content is low relative to other components such as quartz, the overall soil spectra may display weaker kaolinite bands (Ma et al., 2024). High levels of soil properties (i.e., sand, clay, SOC, and EC) can suppress or mask other soil properties (Naimi et al., 2022; O'Rourke, Stockmann et al., 2016). Another difficulty is to compare complete one soil profile spectra to another since they have many horizons. Vasques et al. (2015) evaluated 200 profiles and developed a technique where the spectra of all horizons were analyzed simultaneously and reached 69% agreement between spectroscopy and manual soil classification. Poppiel et al. (2016) concluded that the identification of soil and landscape relationships was fundamental for understanding pedogenetic processes along the toposequences, since the role of relief in the soil evolution of the studied area is extremely important.

Regardless of soil types, spectroscopy may include the soil weathering evaluation as performed by Demattê and da Silva Terra (2014). The authors observed that different weathering levels and, consequently, soil formation processes alter the soils along a toposequence, which reflects on their spectral behavior. D. C. Mello et al. (2023) used a combined field and laboratory sensors employing Vis-NIR, MIR, and pXRF spectroscopy and could identify diagnostic soil horizons and their properties. In addition, our results suggest that in situ sensor-based field measurements would be highly complementary to conventional methods. Dotto et al. (2020) went further and proposed a method to classify soils based on spectral patterns. These findings highlight the potential for new approaches to enhance soil visualization and understanding in the field.

4.2.4 | Soil horizon and depth

Soil horizons boundaries are delineated by soil morphological properties (Soil Survey Staff, 2014). Soil spectroscopy can help to discern differences among pedogenetic features related to master (O, A, B, C, and E horizons) and horizon suffixes (b, g, k, t, ss, x, and w) (Mancini et al., 2021; Viscarra Rossel et al., 2009; Weindorf et al., 2012; Zhang et al., 2021; Zhu et al., 2011). Zhang and Hartemink (2021) focused on the short-range variation of sand, silt, clay, and TC in the soil profiles including A, B, and C horizons of Alfisols, Mollisols, and Entisols. They reported that these soil properties had a higher variation in B and C horizons compared to A horizons. They also found that short-range variation was more affected by parent material than by differences in land use.

Soil horizons have different spectral patterns (Benedet et al., 2020; Zhang et al., 2021). Gozukara, Akça et al. (2022) focused on the effect of individual or combined A and B horizons in the prediction model of sand, silt, clay, TC, and pH using Vis-NIR and pXRF spectra. They found that Vis-NR spectra can be used to achieve higher prediction accuracy to predict clay ($R^2 = 0.84$) in A horizons, TC ($R^2 = 0.91$) in A + B horizons, and pH ($R^2 = 0.79$) in A horizons, whereas pXRF spectra had better prediction accuracy in the prediction of sand ($R^2 = 0.97$) and silt ($R^2 = 0.94$) in B horizons. Andrade, Silva, Faria et al. (2020) achieved relatively higher prediction accuracy for clay ($R^2 = 0.71$) and silt ($R^2 = 0.44$), whereas sand ($R^2 = 0.79$) content was not affected by the splitting of soil horizons (individually using A and B horizons).

Xian-li et al. (2012) found that the prediction accuracy of SOM and pH was mainly affected by soil depth (0–20 cm and 40–60 cm) using Vis-NIR spectra. For example, they reported that the prediction accuracies of SOM were $R^2 = 0.24$ for 0- to 20-cm depth and $R^2 = 0.77$ for 40- to 60-cm depth, whereas the prediction accuracies of pH were $R^2 = 0.00$ for 0- to 20-cm depth and $R^2 = 0.48$ for 40- to 60-cm depth. Coblinski et al. (2020) focused on three different soil depths (0–20 cm, 20–40 cm, and 40–60 cm) to explore their effects on the prediction of sand, silt, and clay using Vis-NIR and MIR spectroscopy. The prediction accuracies of sand, silt, and clay were considerably affected by depth for Vis-NIR ($R^2 = 0.68$–0.84, 0.55–0.74, and 0.10–0.21, respectively) and MIR ($R^2 = 0.57$–0.76, 0.01–0.30, and 0.80–0.93, respectively) spectroscopy. Gozukara, Altunbas et al. (2022), Gozukara, Zhang et al. (2022), and Gozukara, Akça et al. (2022) pointed out that the difference in soil depth (0–20 cm and 0–100 cm) had a considerable effect on the prediction accuracy of sand ($R^2 = 0.56$–0.84), silt ($R^2 = 0.47$–0.55), clay ($R^2 = 0.61$–0.80), EC ($R^2 = 0.33$–0.93), and pH ($R^2 = 0.19$–0.81) using pXRF and Vis-NIR spectra.

These variations in the prediction accuracy for soil physical and chemical properties with horizons/depths may be explained by differences in soil color based on drainage conditions (poorly or moderately), mineralogy (i.e., hematite, quartz, and calcite), and soil properties. Different horizons (i.e., argillic, albic, calcic, gypsic, natric, spodic, and salic) have unique soil physical, chemical, and mineralogical soil properties. Some features (i.e., sand, clay, SOM, and EC) can suppress or mask the other soil properties. Naimi et al. (2022) reported that the absorption peak at 2338 nm of carbonate in the Vis-NIR region disappeared due to the higher content of gypsum. Zhang and Hartemink (2020) pointed out that the prediction accuracies of TC and TN were affected by particle size. O'Rourke, Stockmann et al. (2016) highlighted that prediction of soil geochemistry may be affected by the masking effect of a high concentration of SOC. Knadel et al. (2018) showed that fine mineral particles can mask other soil properties, making it harder to predict characteristics like clay and specific surface area with Vis-NIR spectroscopy. They found that non-complexed organic carbon on mineral surfaces affects the spectral response. Additionally, clay may obscure other soil features due to its strong absorption properties, which highlights the limitation of spectroscopy in soil analysis. Sørensen and Dalsgaard (2005) and Davari et al. (2021) mentioned the same findings related to the masking effects of high clay content on other soil properties, including silt, sand, and SOM/SOC, which resulted in lower prediction accuracy for these soil properties. This masking effect of clay may be more severe in Bt horizons, which contain high amounts of clay.

4.3 | Prediction accuracy of pXRF, MIR, and Vis-NIR spectra for soil properties

The pXRF spectrometer provides elemental concentrations and spectra and the soil spectra can predict some soil properties indirectly, as these properties often correlate with specific elemental concentrations (S. H. G. Silva et al., 2021). For example, soil texture, CEC, and EC are influenced by elements like calcium, magnesium, and potassium, which can be accurately measured using pXRF (O'Rourke, Minasny et al., 2016). However, the prediction accuracy of pXRF spectra can be lower compared to MIR and Vis-NIR spectra.

MIR spectroscopy provides relatively high prediction accuracy due to its rich spectral information and direct sensitivity to chemical bonds, making it superior to VIS-NIR and pXRF in many applications. MIR spectra contain distinct absorption bands that correspond to organic material, such as alkyl (C–H, 2930 and 2850 cm^{-1}); carboxylic acids (C = O, 1725 cm^{-1}); amides (C = O, 1640 cm^{-1}); aromatics (C = C, 1510 cm^{-1}); methyls (C–H, 1445–1350 cm^{-1}); phenolics (C–OH, 1275 cm^{-1}); carbohydrates (C–O, 1050 cm^{-1}) (Nkwain et al., 2018; Viscarra Rossel & Behrens 2010). An absorption peak at 2517 cm^{-1} is associated with the presence of $CaCO_3$ (Hutengs et al., 2019). Additionally, absorption peaks in the range of 1280–1070 cm^{-1} corresponded to silicates (Si–O) (Hutengs et al., 2019), while the peak near 916 cm^{-1} was indicative of Al–OH bonds in clay minerals (Nayak & Singh, 2007). Clay minerals also exhibit characteristic absorption bands including, O–H stretching at 3695 and 3620 cm^{-1}, Si–O stretching at 1280–1070 cm^{-1}, Al–OH at 916 cm^{-1}, and coupled Al–O and Si–O vibrations at 626 cm^{-1} (Madejová & Komadel, 2001; Nayak & Singh, 2007; Nguyen et al., 1991; Viscarra Rossel & Behrens, 2010). Quartz is identified by Si–O vibrations in the ranges of 2000–1650 cm^{-1} and at specific peaks of 811, 790, and 693 cm^{-1} (Churchman et al., 2010; Nayak & Singh, 2007; Nguyen et al., 1991), while water shows O–H stretching at 1633 cm^{-1} (Madejová & Komadel, 2001). These well-defined bands in MIR region allow high prediction and characterization accuracy of critical soil properties compared to Vis-NIR spectra.

Vis-NIR detects overtones and combination bands of basic vibrations, which are less specific and frequently overlap considerably. This reduces the resolution of spectral features, making it difficult to accurately link spectral data with specific soil properties. However, MIR spectra directly catch fundamental vibrations with more specificity and clearer spectrum signals for critical soil properties such as SOC, carbonates, and clays (Pirie et al., 2005). Additionally, the spectral range of Vis-NIR (350–2500 nm) is lower than the spectral range of MIR (2500–25,000 nm). This limited information density and specificity may be related to the relatively low prediction accuracy for some soil physical and chemical properties when using Vis-NIR spectra. Santos et al. (2020), using MIR, reached an important R^2 of 0.86 and 0.97 for SOC and nitrogen, respectively. Moura-Bueno et al. (2018) observed that predictive models can be improved when the variation in soil characteristics is considered, underscoring the need for a preliminary study examining the grouping of the sample set to validate the use of local spectral libraries for the prediction of soil properties.

5 | FUTURE NEEDS

In 2013, a meeting entitled "Soil Spectroscopy: the Present and Future of Soil Monitoring" was held in Rome, Italy, at the Food and Agriculture Organization (FAO). The importance of using soil spectroscopy for the worldwide community had been realized and Ben Dor et al. (2015) develop the a protocol on how to prepare samples and calibrate sensors. This was tested and achieved good results (Romero et al., 2018) which should be followed by regulation of the protocol and instrumentation. This is an ongoing initiative described in Ben Dor et al. (2024).

There is an increasing demand for soil analysis due to the growing need for food production and environmental assessment. More soil samples can be taken for which less traditional soil analysis is needed. For example, Ramirez-Lopez et al. (2018), scanned 910 soil samples using Vis-NIR, and observed that 26% of them should be sent for traditional soil analysis. As a next step, an unprecedent free-cloud-based platform was created (Demattê et al., 2022; besbbr.com.br). In this process, the user sent the spectra of Vis-NIR or MIR of their soil sample to the cloud, which is modeled, and soil analyses are sent by email.

Another topic is that most studies go after correlation and statistical results for quantification of soil attributes. This approach has achieved great results but left behind an explanation of the results. To respond to this question, basic science must re-start as it was in the initial of spectroscopy background. Examples can be seen in Silvero et al. (2020) who explained what was happening in the spectra regarding mineralogy, carbon, and moisture. Demattê, Ramirez-Lopez et al. (2017) developed a understanding of soil type, mineralogy, and chemistry, specifically highlighting how elements such as K and Mg affect spectral results due to their atomic structure. It is not possible to go forward without this type of more fundamental understanding. Therefore, it is recommended to evaluate the spectrum with an expert before and/or alongside a statistical approach. This was observed by Ma et al. (2023), in which "the combination of machine learning and domain knowledge is recommended to develop more meaningful models for the predicting soil properties within the field of soil science."

6 | CONCLUSIONS

We reviewed 305 papers that used Vis-NIR, MIR, and pXRF spectra to predict soil physical and chemical properties, including sand, silt, clay, TN, TC, SIC, SOC, SOM, CEC, EC, pH, and $CaCO_3$. The following can be concluded:

1. Variation in prediction accuracy is caused by soil factors (horizon/depth) and researcher based factors (type or brand of spectrometers, which differ in hardware, spectral range, resolution, and calibration protocols, preprocessing methods, prediction models, and soil analysis methods for calibration).
2. There is an increasing number of soil studies using Vis-NIR, MIR, and pXRF spectra.
3. More than half of the studies focused on the prediction of TC/SIC/SOC/SOM using Vis-NIR spectra.
4. The number of papers related to MIR spectra is fewer than Vis-NIR spectra but more than pXRF. In fact, the number of soil samples used in the prediction model becomes lower on sequence Vis-NIR, MIR, and pXRF, which is related to operational difficulties.
5. About 21% of the papers in soil spectroscopy lack the mention of soil classification.
6. Higher prediction accuracy for SIC, TC, CEC, SOM, clay, sand, SOC, TN, and pH is obtained using the MIR spectrometer. Vis-NIR and pXRF can be used to predict EC and silt and $CaCO_3$.
7. Most papers used fixed soil depth (i.e., 0–20 cm, 0–30 cm, and 20–40 cm) instead of soil genetic horizons to collect soil samples.
8. The number of soil samples used in the prediction model with pXRF spectra was less than Vis-NIR and MIR spectra.
9. The spectral range used in the prediction model was related to researcher preference (i.e., remove noise and selection of spectral range) and the capability of Vis-NIR and MIR spectrometers.
10. Partial least square regression was mostly used in the prediction of soil properties using Vis-NIR and MIR, whereas RF was mostly utilized using pXRF. Prediction models affected the prediction accuracy.
11. Soil analytical methods affect the prediction accuracy for soil properties, in particular soil texture, EC, and pH.

AUTHOR CONTRIBUTIONS

Gafur Gozukara: Conceptualization; data curation; formal analysis; investigation; methodology; resources; software; supervision; validation; visualization; writing—original draft; writing—review and editing. **Alfred E. Hartemink**: Conceptualization; data curation; formal analysis; investigation; methodology; resources; supervision; validation; visualization; writing—original draft; writing—review and editing. **Jingyi Huang**: Methodology; supervision; writing—original draft; writing—review and editing. **José Alexandre Melo Demattê**: Methodology; supervision; writing—original draft; writing—review and editing.

ACKNOWLEDGMENTS

The first author would like to thank Eskisehir Osmangazi University Scientific Research Projects Coordination Unit under grant numbers 201923025 in 2019 and FUİ-2022-2318 in 2022. These scholarships were provided to the first author to explore the relationship between soil and Vis-NIR, MIR, and pXRF spectra and to build the collaboration for this review paper with University of Wisconsin-Madison, Department of Soil Science, FD Hole Soils Lab.

CONFLICT OF INTEREST STATEMENT

The authors declare no conflicts of interest.

ORCID

Gafur Gozukara https://orcid.org/0000-0003-0940-5218
Alfred E. Hartemink https://orcid.org/0000-0002-5797-6798
Jingyi Huang https://orcid.org/0000-0002-1209-9699
José Alexandre Melo Demattê https://orcid.org/0000-0001-5328-0323

REFERENCES

Acree, A., Weindorf, D. C., Paulette, L., Van Gestle, N., Chakraborty, S., Man, T., Jordan, C., & Prieto, J. L. (2020). Soil classification in Romanian catenas via advanced proximal sensors. *Geoderma*, *377*, 114587. https://doi.org/10.1016/j.geoderma.2020.114587

Ahmadi, A., Emami, M., Daccache, A., & He, L. (2021). Soil properties prediction for precision agriculture using visible and near-infrared spectroscopy: A systematic review and meta-analysis. *Agronomy*, *11*(3), 433. https://doi.org/10.3390/agronomy11030433

Andrade, R., Silva, S. H. G., Faria, W. M., Poggere, G. C., Barbosa, J. Z., Guilherme, L. R. G., & Curi, N. (2020). Proximal sensing applied to soil texture prediction and mapping in Brazil. *Geoderma Regional*, *23*, e00321. https://doi.org/10.1016/j.geodrs.2020.e00321

Andrade, R., Silva, S. H. G., Weindorf, D. C., Chakraborty, S., Faria, W. M., Guilherme, L. R. G., & Curi, N. (2020). Tropical soil order and suborder prediction combining optical and X-ray approaches. *Geoderma Regional*, *23*, e00331. https://doi.org/10.1016/j.geodrs.2020.e00331

Andrade, R., Silva, S. H. G., Weindorf, D. C., Chakraborty, S., Faria, W. M., Mesquita, L. F., Guilherme, L. R. G., & Curi, N. (2020). Assessing models for prediction of some soil chemical properties from portable X-ray fluorescence (pXRF) spectrometry data in Brazilian Coastal Plains. *Geoderma*, *357*, 113957. https://doi.org/10.1016/j.geoderma.2019.113957

Araujo, M. A., Pedroso, A. V., Amaral, D. C., & Zinn, Y. L. (2014). Paragênese mineral de solos desenvolvidos de diferentes litologias na região sul de Minas Gerais. *Revista Brasileira de Ciência Do Solo*, *38*, 11–25. https://doi.org/10.1590/S0100-06832014000100002

Barthès, B. G., Kouakoua, E., Coll, P., Clairotte, M., Moulin, P., Saby, N. P., Le Cadre, E., Etayo, A., & Chevallier, T. (2020). Improvement in spectral library-based quantification of soil properties using representative spiking and local calibration—The case of soil inorganic carbon prediction by mid-infrared spectroscopy. *Geoderma*, *369*, 114272. https://doi.org/10.1016/j.geoderma.2020.114272

Bellon-Maurel, V., & McBratney, A. (2011). Near-infrared (NIR) and mid-infrared (MIR) spectroscopic techniques for assessing the amount of carbon stock in soils—Critical review and research perspectives. *Soil Biology & Biochemistry*, *43*(7), 1398–1410. https://doi.org/10.1016/j.soilbio.2011.02.019

Ben-Dor, E., Inbar, Y., & Chen, Y. (1997). The reflectance spectra of organic matter in the visible near-infrared and short wave infrared region (400–2500 nm) during a controlled decomposition process. *Remote Sensing of Environment*, *61*(1), 1–15. https://doi.org/10.1016/S0034-4257(96)00120-4

Ben Dor, E., Karyotis, K., Chabrillat, S., & Schmid, T. (2024). Standardization and protocol development for soil spectral reflectance in laboratory and field settings: An overview of IEEE SA P4005 activity. In *IGARSS 2024-2024 IEEE international geoscience and remote sensing symposium* (pp. 268–270). Institute of Electrical and Electronics Engineers Inc.

Ben Dor, E., Ong, C., & Lau, I. C. (2015). Reflectance measurements of soils in the laboratory: Standards and protocols. *Geoderma*, *245*, 112–124. https://doi.org/10.1016/j.geoderma.2015.01.002

Benedet, L., Faria, W. M., Silva, S. H. G., Mancini, M., Guilherme, L. R. G., Demattê, J. A. M., & Curi, N. (2020). Soil subgroup prediction via portable X-ray fluorescence and visible near-infrared spectroscopy. *Geoderma*, *365*, 114212. https://doi.org/10.1016/j.geoderma.2020.114212

Benedet, L., Silva, S. H. G., Mancini, M., dos Santos Teixeira, A. F., Inda, A. V., Demattê, J. A., & Curi, N. (2022). Variation of properties of two contrasting Oxisols enhanced by pXRF and Vis-NIR. *Journal of South American Earth Sciences*, *115*, 103748. https://doi.org/10.1016/j.jsames.2022.103748

Bigham, J. M., Fitzpatrick, R. W., & Schulze, D. G. (2002). Iron oxides. In J. B. Dixon & D. G. Schulze (Eds.), *Soil mineralogy with environmental applications* (Vol. 7, pp. 323–366). Soil Science Society of America. https://doi.org/10.2136/sssabookser7.c10

Chang, C. W., Laird, D. A., & Hurburgh Jr, C. R. (2005). Influence of soil moisture on near-infrared reflectance spectroscopic measurement of soil properties. *Soil Science*, *170*(4), 244–255. https://doi.org/10.1097/01.ss.0000162289.40879.7b

Chen, S., Arrouays, D., Mulder, V. L., Poggio, L., Minasny, B., Roudier, P., Libohova, Z., Lagacherie, P., Shi, Z., Hannam, J., Meersmans, J., Richer-de-Forges, A. C., & Walter, C. (2022). Digital mapping of GlobalSoilMap soil properties at a broad scale: A review. *Geoderma*, *409*, 115567. https://doi.org/10.1016/j.geoderma.2021.115567

Chevallier, T., Fujisaki, K., Roupsard, O., Guidat, F., Kinoshita, R., de Melo Viginio Filho, E., Lehner, P., & Albrecht, A. (2019). Short-range-order minerals as powerful factors explaining deep soil organic carbon stock distribution: The case of a coffee agroforestry plantation on Andosols in Costa Rica. *Soilless*, *5*(2), 315–332. https://doi.org/10.5194/soil-5-315-2019

Churchman, G. J., Foster, R. C., D'Acqui, L. P., Janik, L. J., Skjemstad, J. O., Merry, R. H., & Weissmann, D. A. (2010). Effect of land-use history on the potential for carbon sequestration in an Alfisol. *Soil & Tillage Research*, *109*(1), 23–35. https://doi.org/10.1016/j.still.2010.03.012

Coblinski, J. A., Giasson, É., Demattê, J. A., Dotto, A. C., Costa, J. J. F., & Vašát, R. (2020). Prediction of soil texture classes through different wavelength regions of reflectance spectroscopy at various soil depths. *Catena*, *189*, 104485. https://doi.org/10.1016/j.catena.2020.104485

Cobo, J. G., Dercon, G., Yekeye, T., Chapungu, L., Kadzere, C., Murwira, A., Delve, R., & Cadisch, G. (2010). Integration of mid-infrared spectroscopy and geostatistics in the assessment of soil spatial variability at landscape level. *Geoderma*, *158*(3–4), 398–411. https://doi.org/10.1016/j.geoderma.2010.06.013

Conyers, M. K., Poile, G. J., Oates, A. A., Waters, D., & Chan, K. Y. (2011). Comparison of three carbon determination methods on naturally occurring substrates and the implication for the quantification of "soil carbon". *Soil Research*, *49*, 27–33. https://doi.org/10.1071/SR10103

Çullu, M. A., Şeker, H., Gozukara, G., Günal, H., & Bilgili, A. V. (2024). Rapid characterization of soil horizons for different soil series utilizing Vis-NIR spectral information. *Geoderma Regional*, *38*, e00853. https://doi.org/10.1016/j.geodrs.2024.e00853

Curi, N., & Franzmeier, D. P. (1987). Effect of parent rocks on chemical and mineralogical properties of some Oxisols in Brazil. *Soil Science Society of America Journal*, *51*, 153–158. https://doi.org/10.2136/sssaj1987.03615995005100010033x

Dangal, S. R., Sanderman, J., Wills, S., & Ramirez-Lopez, L. (2019). Accurate and precise prediction of soil properties from a large mid-infrared spectral library. *Soil Systems*, *3*(1), 11. https://doi.org/10.3390/soilsystems3010011

Davari, M., Karimi, S. A., Bahrami, H. A., Hossaini, S. M. T., & Fahmideh, S. (2021). Simultaneous prediction of several soil properties related to engineering uses based on laboratory Vis-NIR reflectance spectroscopy. *Catena*, *197*, 104987. https://doi.org/10.1016/j.catena.2020.104987

Davies, B. E. (1971). A statistical comparison of pH values of some English soils after measurement in both water and 0.01 M calcium chloride. *Soil Science Society of America Journal*, *35*, 551–552. https://doi.org/10.2136/sssaj1971.03615995003500040022x

de Faria, A. J. G., Silva, S. H. G., Andrade, R., Mancini, M., Melo, L. C. A., Weindorf, D. C., Guilherme, L. G. G., & Curi, N. (2022). Prediction of soil organic matter content by combining data from Nix ProTM color sensor and portable X-ray fluorescence spectrometry in tropical soils. *Geoderma Regional*, *28*, e00461. https://doi.org/10.1016/j.geodrs.2021.e00461

Demattê, J. A. M., Bellinaso, H., Romero, D. J., & Fongaro, C. T. (2014). Morphological interpretation of reflectance spectrum (MIRS) using libraries looking towards soil classification. *Scientia Agricola*, *71*, 509–520. https://doi.org/10.1590/0103-9016-2013-0365

Demattê, J. A. M., & da Silva Terra, F. (2014). Spectral pedology: A new perspective on evaluation of soils along pedogenetic alterations. *Geoderma*, *217–218*, 190–200. https://doi.org/10.1016/j.geoderma.2013.11.012

Demattê, J. A. M., Dotto, A. C., Bedin, L. G., Sayão, V. M., & e Souza, A. B. (2019a). Soil analytical quality control by traditional and spectroscopy techniques: Constructing the future of a hybrid laboratory for low environmental impact. *Geoderma*, *337*, 111–121. https://doi.org/10.1016/j.geoderma.2018.09.010

Demattê, J. A. M., Dotto, A. C., Paiva, A. F. S., Sato, M. V., Dalmolin, R. S. D., de Araújo, M. D. S. B., da Silva, E. B., Nanni, M. R., ten Caten, A., Noronha, N. C., Lacerda, M. P. C., de Araújo Filho, J. C., Rizzo, R., Bellinaso, H., Francelino, M. R., Schaefer, C. E. G. R., Vicente, L. E., dos Santos, U. J., de S´a Barretto Sampaio, E. V., … do Couto, H. T. Z. (2019b). The Brazilian Soil Spectral Library (BSSL): A general view, application and challenges. *Geoderma*, *354*, 113793. https://doi.org/10.1016/j.geoderma.2019.05.043

Demattê, J. A. M., Horák-Terra, I., Beirigo, R. M., da Silva Terra, F., Marques, K. P. P., Fongaro, C. T., Silva, A. C., & Vidal-Torrado, P. (2017). Genesis and properties of wetland soils by VIS-NIR-SWIR as a technique for environmental monitoring. *Journal of Environmental Management*, *197*, 50–62. https://doi.org/10.1016/j.jenvman.2017.03.014

Demattê, J. A. M., Paiva, A. F. S., Rosin, N. A., Ruiz, L. F. C., Poppiel, R. R., Mello, F. A., Minasny, B., Grunwald, S., Chabrillat, S., Francos, N., Ge, Y., Ben Dor, E., Gholizadeh, A., Gomez, C., Ayoubi, S., Fiantis, D., Biney, J. K. M., Wang, C., Belal, A., … Silvero, N. E. Q. (2022). The Brazilian Soil Spectral Service (BraSpecS): A user-friendly system for global soil spectra communication. *Remote Sensing*, *14*, 740. https://doi.org/10.3390/rs14030740

Demattê, J. A. M., Ramirez-Lopez, L., Marques, K. P. P., & Rodella, A. A. (2017). Chemometric soil analysis on the determination of specific bands for the detection of magnesium and potassium by spectroscopy. *Geoderma*, *288*, 8–22. https://doi.org/10.1016/j.geoderma.2016.11.013

de Santana, F. B., Grunsky, E. C., Fitzsimons, M. M., Gallagher, V., & Daly, K. (2022). Diffuse reflectance mid infra-red spectroscopy combined with machine learning algorithms can differentiate spectral signatures in shallow and deeper soils for the prediction of pH and organic matter content. *Catena*, *218*, 106552. https://doi.org/10.1016/j.catena.2022.106552

Di lorio, E., Napoletano, P., Circelli, L., Memoli, V., Santorufo, L., De Marco, A., & Colombo, C. (2022). Comparison of natural and technogenic soils developed on volcanic ash by Vis-NIR spectroscopy. *Catena*, *216*, 106369. https://doi.org/10.1016/j.catena.2022.106369

Dotto, A. C., Dalmolin, R. S. D., Grunwald, S., ten Caten, A., & Pereira Filho, W. (2017). Two preprocessing techniques to reduce model covariables in soil property predictions by Vis-NIR spectroscopy. *Soil & Tillage Research*, *172*, 59–68. https://doi.org/10.1016/j.still.2017.05.008

Dotto, A. C., Dalmolin, R. S. D., ten Caten, A., & Grunwald, S. (2018). A systematic study on the application of scatter-corrective and spectral-derivative preprocessing for multivariate prediction of soil organic carbon by Vis-NIR spectra. *Geoderma*, *314*, 262–274. https://doi.org/10.1016/j.geoderma.2017.11.006

Dotto, A. C., Demattê, J. A. M., Viscarra Rossel, R., & Rizzo, R. (2020). Soil environment grouping system based on spectral, climate, and terrain data: A quantitative branch of soil series. *Soilless*, *6*, 163–177. https://doi.org/10.5194/soil-6-163-2020

Duda, B. M., Weindorf, D. C., Chakraborty, S., Li, B., Man, T., Paulette, L., & Deb, S. (2017). Soil characterization across catenas via advanced proximal sensors. *Geoderma*, *298*, 78–91. https://doi.org/10.1016/j.geoderma.2017.03.017

Dunn, B. W., Beecher, H. G., Batten, G. D., & Ciavarella, S. (2002). The potential of near infrared reflectance spectroscopy for soil analysis—A case study from the Riverine Plain of south-eastern Australia. *Australian Journal of Experimental Research*, *42*, 607–614. https://doi.org/10.1071/EA01172

Fitzpatrick, R. W., & Schwertmann, U. V. (1982). Al-substituted goethite—an indicator of pedogenic and other weathering environments in South Africa. *Geoderma*, *27*(4), 335–347. https://doi.org/10.1016/0016-7061(82)90022-2

Gómez, A. M., Albarracin, H. S. R., de Mello, D. C., Silvero, N. E., Rosin, N. A., Bellinaso, H., Fernandes-Filho, E. I., Veloso, G. V., Greschuk, L. T., Savin, I., Araujo, M. S., Souza, S. F. F., & Dematte, J. A. (2022). Proximal sensing approach for soil characterization and discrimination: A case of study in Brazil. *Geocarto International*, *37*(27), 15806–15822. https://doi.org/10.1080/10106049.2022.2102228

Gozukara, G., Acar, M., Ozlu, E., Dengiz, O., Hartemink, A. E., & Zhang, Y. (2022). A soil quality index using Vis-NIR and pXRF spectra of a soil profile. *Catena*, *211*, 105954. https://doi.org/10.1016/j.catena.2021.105954

Gozukara, G., Akça, E., Dengiz, O., Kapur, S., & Adak, A. (2022). Soil particle size prediction using Vis-NIR and pXRF spectra in a semiarid agricultural ecosystem in Central Anatolia of Türkiye. *Catena*, *217*, 106514. https://doi.org/10.1016/j.catena.2022.106514

Gozukara, G., Altunbas, S., Dengiz, O., & Adak, A. (2022). Assessing the effect of soil to water ratios and sampling strategies on the prediction of EC and pH using pXRF and Vis-NIR spectra. *Computers and Electronics in Agriculture*, *203*, 107459. https://doi.org/10.1016/j.compag.2022.107459

Gozukara, G., Zhang, Y., & Hartemink, A. E. (2021). Using vis-NIR and pXRF data to distinguish soil parent materials—An example using 136 pedons from Wisconsin, USA. *Geoderma*, *396*, 115091. https://doi.org/10.1016/j.geoderma.2021.115091

Gozukara, G., Zhang, Y., & Hartemink, A. E. (2022). Using pXRF and vis-NIR spectra for predicting properties of soils developed in loess. *Pedosphere*, *32*(4), 602–615. https://doi.org/10.1016/S1002-0160(21)60092-9

Gras, J. P., Barthès, B. G., Mahaut, B., & Trupin, S. (2014). Best practices for obtaining and processing field visible and near infrared (VNIR) spectra of topsoils. *Geoderma*, *214*, 126–134. https://doi.org/10.1016/j.geoderma.2013.09.021

Grauer-Gray, J., & Hartemink, A. E. (2018). Raster sampling of soil profiles. *Geoderma*, *318*, 99–108. https://doi.org/10.1016/j.geoderma.2017.12.029

Greenberg, I., Seidel, M., Vohland, M., Koch, H. J., & Ludwig, B. (2022). Performance of in situ vs laboratory mid-infrared soil spectroscopy using local and regional calibration strategies. *Geoderma*, *409*, 115614. https://doi.org/10.1016/j.geoderma.2021.115614

Greschuk, L. T., Demattê, J. A., Silvero, N. E., & Rosin, N. A. (2023). A soil productivity system reveals most Brazilian agricultural lands are below their maximum potential. *Scientific Reports*, *13*(1), 14103. https://doi.org/10.1038/s41598-023-39981-y

Grinand, C., Barthès, B. G., Brunet, D., Kouakoua, E., Arrouays, D., Jolivet, C., Caria, G., & Bernoux, M. (2012). Prediction of soil organic and inorganic carbon contents at a national scale (France) using mid-infrared reflectance spectroscopy (MIRS). *European Journal of Soil Science*, *63*(2), 141–151. https://doi.org/10.1111/j.1365-2389.2012.01429.x

Haghi, R. K., Pérez-Fernández, E., & Robertson, A. H. J. (2021). Prediction of various soil properties for a national spatial dataset of Scottish soils based on four different chemometric approaches: A comparison of near infrared and mid-infrared spectroscopy. *Geoderma*, *396*, 115071. https://doi.org/10.1016/j.geoderma.2021.115071

Hammes, K., Schmidt, M. W. I., Smernik, R. J., Currie, L. A., Ball, W. P., Nguyen, T. H., Louchouarn, P., Houel, S., Gustafsson, O., Elmquist, M., Cornelissen, G., Skjemstad, J. O., Masiello, C. A., Song, J., Peng, P., Mitra, S., Dunn, J. C., Hatcher, P. G., Hockaday, W. C., … Ding, L. (2007). Comparison of quantification methods to measure fire-derived (black-elemental) carbon in soils and sediments using reference materials from soil, water, sediment and the atmosphere. *Global Biogeochemical Cycles*, *21*(3), GB3016. https://doi.org/10.1029/2006GB002914

Hayes, M. H. (1996). *Statistical digital signal processing and modeling*. Wiley.

Hong, Y., Chen, Y., Chen, S., Shen, R., Hu, B., Peng, J., Wang, N., Guo, L., Zhuo, Z., Yang, Y., Liu, Y., Moıazen, A. M., & Shi, Z. (2022). Data mining of urban soil spectral library for estimating organic carbon. *Geoderma*, *426*, 116102. https://doi.org/10.1016/j.geoderma.2022.116102

Hong, Y., Munnaf, M. A., Guerrero, A., Chen, S., Liu, Y., Shi, Z., & Mouazen, A. M. (2022). Fusion of visible-to-near-infrared and mid-infrared spectroscopy to estimate soil organic carbon. *Soil & Tillage Research*, *217*, 105284. https://doi.org/10.1016/j.still.2021.105284

Hu, J., Huang, Z., Li, S., Liu, B., & Ci, E. (2023). Assessing profile uniformity of soils from weathered clastic sedimentary rocks in southwest China. *Catena*, *224*, 107007. https://doi.org/10.1016/j.catena.2023.107007

Hutengs, C., Eisenhauer, N., Schaedler, M., Lochner, A., Seidel, M., & Vohland, M. (2021). VNIR and MIR spectroscopy of PLFA-derived soil microbial properties and associated soil physicochemical characteristics in an experimental plant diversity gradient. *Soil Biology & Biochemistry*, *160*, 108319. https://doi.org/10.1016/j.soilbio.2021.108319

Hutengs, C., Seidel, M., Oertel, F., Ludwig, B., & Vohland, M. (2019). In situ and laboratory soil spectroscopy with portable visible-to-near-infrared and mid-infrared instruments for the assessment of organic carbon in soils. *Geoderma*, *355*, 113900. https://doi.org/10.1016/j.geoderma.2019.113900

İnci, Y., Bilgili, A. V., Gündoğan, R., Gözükara, G., Karadağ, K., & Tenekeci, M. E. (2024). Machine learning-based classification of soil parent materials using elemental concentration and Vis-NIR data. *Sensors*, *24*(16), 5126. https://doi.org/10.3390/s24165126

Jenny, H. (1941). *Factors of soil formation: A system of quantitative pedology*. McGraw-Hill Book Co., Inc.

Jiang, Z., Liu, Q., Colombo, C., Barrón, V., Torrent, J., & Hu, P. (2014). Quantification of Al-goethite from diffuse reflectance spectroscopy and magnetic methods. *Geophysical Journal International*, *196*(1), 131–144. https://doi.org/10.1093/gji/ggt377

John, K., Kebonye, N. M., Agyeman, P. C., & Ahado, S. K. (2021). Comparison of Cubist models for soil organic carbon prediction via portable XRF measured data. *Environmental Monitoring and Assessment*, *193*, Article 197. https://doi.org/10.1007/s10661-021-08946-x

Knadel, M., Arthur, E., Weber, P., Moldrup, P., Greve, M. H., Chrysodonta, Z. P., & De Jonge, L. W. (2018). Soil specific surface area determination by visible near-infrared spectroscopy. *Soil Science Society of America Journal*, *82*(5), 1046–1056. https://doi.org/10.2136/sssaj2018.03.0093

Knadel, M., Stenberg, B., Deng, F., Thomsen, A., & Greve, M. H. (2013). Comparing predictive abilities of three visible-near infrared spectrophotometers for soil organic carbon and clay determination. *Journal of Near Infrared Spectroscopy*, *21*(1), 67–80. https://doi.org/10.1255/jnirs.1035

Kuang, B., & Mouazen, A. M. (2012). Influence of the number of samples on prediction error of visible and near-infrared spectroscopy of selected soil properties at the farm scale. *European Journal of Soil Science*, *63*(3), 421–429. https://doi.org/10.1111/j.1365-2389.2012.01456.x

Leue, M., Hoffmann, C., Hierold, W., & Sommer, M. (2019). In-situ multi-sensor characterization of soil cores along an erosion-deposition gradient. *Catena*, *182*, 104140. https://doi.org/10.1016/j.catena.2019.104140

Levi, N., Karnieli, A., & Paz-Kagan, T. (2020). Using reflectance spectroscopy for detecting land-use effects on soil quality in drylands. *Soil & Tillage Research*, *199*, 104571. https://doi.org/10.1016/j.still.2020.104571

Li, R., Yin, B., Cong, Y., & Du, Z. (2020). Simultaneous prediction of soil properties using multi_cnn model. *Sensors*, *20*(21), 6271. https://doi.org/10.3390/s20216271

Liu, J., Xie, J., Han, J., Wang, H., Sun, J., Li, R., & Li, S. (2020). Visible and near-infrared spectroscopy with chemometrics are able to predict soil physical and chemical properties. *Journal of Soils and Sediments*, *20*, 2749–2760. https://doi.org/10.1007/s11368-020-02623-1

Liu, S., Shen, H., Chen, S., Zhao, X., Biswas, A., Jia, X., Shi, Z., & Fang, J. (2019). Estimating forest soil organic carbon content using vis-NIR spectroscopy: Implications for large-scale soil carbon spectroscopic assessment. *Geoderma*, *348*, 37–44. https://doi.org/10.1016/j.geoderma.2019.04.003

Lucà, F., Conforti, M., Castrignanò, A., Matteucci, G., & Buttafuoco, G. (2017). Effect of calibration set size on prediction at local scale of soil carbon by Vis-NIR spectroscopy. *Geoderma*, *288*, 175–183. https://doi.org/10.1016/j.geoderma.2016.11.015

Ma, Y., Minasny, B., Demattê, J. A., & McBratney, A. B. (2023). Incorporating soil knowledge into machine-learning prediction of soil properties from soil spectra. *European Journal of Soil Science*, *74*(6), e13438. https://doi.org/10.1111/ejss.13438

Ma, Y., Minasny, B., Roudier, P., Theng, B. K., & Carrick, S. (2024). Application of mid-infrared (MIR) spectroscopy to identify and quantify minerals in New Zealand soils. *Catena*, *242*, 108115. https://doi.org/10.1016/j.catena.2024.108115

Madejová, J., & Komadel, P. (2001). Baseline studies of the clay minerals society source clays: Infrared methods. *Clays and Clay Minerals*, *49*, 410–432. https://doi.org/10.1346/CCMN.2001.0490508

Mancini, M., Silva, S. H. G., Avanzi, J. C., Hartemink, A. E., Inda, A. V., Demattê, J. A., Lima, W., & Curi, N. (2023). Digital morphometrics and genesis of soils with buried horizons and lithological discontinuities in southeastern Brazil. *Geoderma Regional*, *32*, e00612. https://doi.org/10.1016/j.geodrs.2023.e00612

Mancini, M., Silva, S. H. G., dos Santos Teixeira, A. F., Guilherme, L. R. G., & Curi, N. (2020). Soil parent material prediction for Brazil via proximal soil sensing. *Geoderma Regional*, *22*, e00310. https://doi.org/10.1016/j.geodrs.2020.e00310

Mancini, M., Silva, S. H. G., Hartemink, A. E., Zhang, Y., de Faria, Á. J. G., Silva, F. M., Inda, A. V., Demattê, J. A. M., & Curi, N. (2021).

Formation and variation of a 4.5 m deep Oxisol in southeastern Brazil. *Catena*, *206*, 105492. https://doi.org/10.1016/j.catena.2021.105492

Mancini, M., Weindorf, D. C., Chakraborty, S., Silva, S. H. G., dos Santos Teixeira, A. F., Guilherme, L. R. G., & Curi, N. (2019). Tracing tropical soil parent material analysis via portable X-ray fluorescence (pXRF) spectrometry in Brazilian Cerrado. *Geoderma*, *337*, 718–728. https://doi.org/10.1016/j.geoderma.2018.10.026

Marques, K. P., Rizzo, R., Dotto, A. C., e Souza, A. B., Mello, F. A., Neto, L. G., Anjos, L. H., & Demattê, J. A. (2019). How qualitative spectral information can improve soil profile classification? *Journal of Near Infrared Spectroscopy*, *27*(2), 156–174. https://doi.org/10.1177/0967033518821965

Mello, D. C., Souza, A. B., Mello, F. A., Marques, K. P., Poppiel, R. R., Belinasso, H., Di Raimo, L. D. L., Francelino, M. R., Fernandes-Filho, E. I., Veloso, G. V., Schaefer, C. E. G. R., & Demattê, J. A. (2023). Sensor-based field methods for pedology and soil surveys: Protocol suggestions for Brazilian tropical soils. *Geoderma Regional*, *33*, e00651. https://doi.org/10.1016/j.geodrs.2023.e00651

Mello, F. A., Bellinaso, H., Mello, D. C., Safanelli, J. L., Mendes, W. D. S., Amorim, M. T., Gomez, A. M. R., Poppiel, R. R., Silverio, N. E. Q., Gholizadeh, A., Silva, S. H. G., Curi, N., & Demattê, J. A. (2021). Soil parent material prediction through satellite multispectral analysis on a regional scale at the Western Paulista Plateau, Brazil. *Geoderma Regional*, *26*, e00412. https://doi.org/10.1016/j.geodrs.2021.e00412

Mendes, W. S., Demattê, J. A., Bonfatti, B. R., Resende, M. E. B., Campos, L. R., & da Costa, A. C. S. (2021). A novel framework to estimate soil mineralogy using soil spectroscopy. *Applied Geochemistry*, *127*, 104909. https://doi.org/10.1016/j.apgeochem.2021.104909

Milinovic, J., Vale, C., & Azenha, M. (2023). Recent advances in multivariate analysis coupled with chemical analysis for soil surveys: A review. *Journal of Soils and Sediments*, *23*(3), 1085–1098. https://doi.org/10.1007/s11368-022-03377-8

Minasny, B., McBratney, A. B., Tranter, G., & Murphy, B. W. (2008). Using soil knowledge for the evaluation of mid-infrared diffuse reflectance spectroscopy for predicting soil physical and mechanical properties. *European Journal of Soil Science*, *59*(5), 960–971. https://doi.org/10.1111/j.1365-2389.2008.01058.x

Minasny, B., Tranter, G., McBratney, A. B., Brough, D. M., & Murphy, B. W. (2009). Regional transferability of mid-infrared diffuse reflectance spectroscopic prediction for soil chemical properties. *Geoderma*, *153*(1–2), 155–162. https://doi.org/10.1016/j.geoderma.2009.07.021

Mirzaeitalarposht, R., & Kambouzia, J. (2020). Development of mid-infrared spectroscopic feature-based indices to quantify soil carbon fractions. *Eurasian Soil Science*, *53*, 73–81. https://doi.org/10.1134/S1064229320010111

Moura-Bueno, J. M., Dalmolin, R. S. D., ten Caten, A., Dotto, A. C., & Demattê, J. A. M. (2018). Stratification of a local VIS-NIR-SWIR spectral library by homogeneity criteria yields more accurate soil organic carbon predictions. *Geoderma*, *337*, 565–581. https://doi.org/10.1016/j.geoderma.2018.10.015

Naimi, S., Ayoubi, S., Di Raimo, L. A. D. L., & Demattê, J. A. M. (2022). Quantification of some intrinsic soil properties using proximal sensing in arid lands: Application of Vis-NIR, MIR, and pXRF spectroscopy. *Geoderma Regional*, *28*, e00484. https://doi.org/10.1016/j.geodrs.2022.e00484

Nawar, S., Buddenbaum, H., Hill, J., Kozak, J., & Mouazen, A. M. (2016). Estimating the soil clay content and organic matter by means of different calibration methods of vis-NIR diffuse reflectance spectroscopy. *Soil & Tillage Research*, *155*, 510–522. https://doi.org/10.1016/j.still.2015.07.021

Nayak, P. S., & Singh, B. K. (2007). Instrumental characterization of clay by XRF, XRD and FTIR. *Bulletin of Materials Science*, *30*(3), 235–238. https://doi.org/10.1007/s12034-007-0042-5

Nduwamungu, C., Ziadi, N., Parent, L. É., Tremblay, G. F., & Thuriès, L. (2009). Opportunities for, and limitations of, near infrared reflectance spectroscopy applications in soil analysis: A review. *Canadian Journal of Soil Science*, *89*(5), 531–541. https://doi.org/10.4141/CJSS08076

Nduwamungu, C., Ziadi, N., Tremblay, G. F., & Parent, L. E. (2009). Near-infrared reflectance spectroscopy prediction of soil properties: Effects of sample cups and preparation. *Soil Science Society of America Journal*, *73*(6), 1896–1903. https://doi.org/10.2136/sssaj2008.0213

Ng, W., Anggria, L., Siregar, A. F., Hartatik, W., Sulaeman, Y., Jones, E., & Minasny, B. (2020). Developing a soil spectral library using a low-cost NIR spectrometer for precision fertilization in Indonesia. *Geoderma Regional*, *22*, e00319. https://doi.org/10.1016/j.geodrs.2020.e00319

Ng, W., Minasny, B., Montazerolghaem, M., Padarian, J., Ferguson, R., Bailey, S., & McBratney, A. B. (2019). Convolutional neural network for simultaneous prediction of several soil properties using visible/near-infrared, mid-infrared, and their combined spectra. *Geoderma*, *352*, 251–267. https://doi.org/10.1016/j.geoderma.2019.06.016

Nguyen, T. T., Janik, L. J., & Raupach, M. (1991). Diffuse reflectance infrared fourier transform (DRIFT) spectroscopy in soil studies. *Australian Journal of Soil Research*, *29*(1), 49–67. https://doi.org/10.1071/SR9910049

Nkwain, F. N., Demyan, M. S., Rasche, F., Dignac, M.-F., Schulz, E., Katterer, T., Müller, T., & Cadisch, G. (2018). Coupling pyrolysis with mid-infrared spectroscopy (Py-MIRS) to fingerprint soil organic matter bulk chemistry. *Journal of Analytical and Applied Pyrolysis*, *133*, 176–184. https://doi.org/10.1016/j.jaap.2018.04.004

Nocita, M., Stevens, A., Toth, G., Panagos, P., van Wesemael, B., & Montanarella, L. (2014). Prediction of soil organic carbon content by diffuse reflectance spectroscopy using a local partial least square regression approach. *Soil Biology & Biochemistry*, *68*, 337–347. https://doi.org/10.1016/j.soilbio.2013.10.022

O'Rourke, S. M., Minasny, B., Holden, N. M., & McBratney, A. B (2016). Synergistic use of Vis-NIR, MIR, and XRF spectroscopy for the determination of soil geochemistry. *Soil Science Society of America Journal*, *80*(4), 888–899. https://doi.org/10.2136/sssaj2015.10.0361

O'Rourke, S. M., Stockmann, U., Holden, N. M., McBratney, A. B., & Minasny, B. (2016). An assessment of model averaging to improve predictive power of portable vis-NIR and XRF for the determination of agronomic soil properties. *Geoderma*, *279*, 31–44. https://doi.org/10.1016/j.geoderma.2016.05.005

Padarian, J., Minasny, B., & McBratney, A. B. (2019). Using deep learning to predict soil properties from regional spectral data. *Geoderma Regional*, *16*, e00198. https://doi.org/10.1016/j.geodrs.2018.e00198

Paiva, A. F. S., Poppiel, R. R., Rosin, N. A., Greschuk, L. T., Rosas, J. T. F., & Demattê, J. A. M. (2022). The Brazilian Program of Soil Analysis via Spectroscopy (ProBASE): Combining spectroscopy and wet laboratories to understand new technologies. *Geoderma*, *421*(1), 115905. https://doi.org/10.1016/j.geoderma.2022.115905

Pirie, A., Singh, B., & Islam, K. (2005). Ultra-violet, visible, near-infrared, and mid-infrared diffuse reflectance spectroscopic techniques to predict several soil properties. *Soil Research*, *43*(6), 713–721. https://doi.org/10.1071/SR04182

Poppiel, R. R., Lacerda, M. P. C., Junior, M. P. O., Demattê, J. A. M., Romero, D. J., Sato, M. V., Almeida Júnior, L. R., & Cassol, L. F. M. (2016). Surface spectroscopy of Oxisols, Entisols and Inceptisol and relationships with selected soil properties. *The Brazilian Journal of Soil Science*, *42*, e0160519. https://doi.org/10.1590/18069657rbcs20160519

Poppiel, R. R., Lacerda, M. P. C., Rizzo, R., Safanelli, J. L., Bonfatti, B. R., Silvero, N. E. Q., & Demattê, J. A. M. (2020). Soil color and mineralogy mapping using proximal and remote sensing in Midwest Brazil. *Remote Sensing*, *12*(7), 1197. https://doi.org/10.3390/rs12071197

Price, T. W., Blevins, R. L., Barnhisel, R. I., & Bailey, H. H. (1975). Lithologic discontinuities in loessial soils of southwestern Kentucky. *Soil Science Society of America Journal*, *39*, 94–98. https://doi.org/10.2136/sssaj1975.03615995003900010026x

Proakis, J. G., & Manolakis, D. G. (2006). *Digital signal preprocessing: Principles, algorithms, and applications*. Pearson Education.

Raimo, L. A. D. L., Couto, E. G., Mello, D. C., Demattê, J. A. M., Amorim, R. S. S., Torres, G. N., Bocuti, E. D., Veloso, G. V., Poppiel, R. R., Francelino, M. R., & Fernandes-Filho, E. L. (2022). Characterizing and modeling tropical sandy soils through VisNIR-SWIR, MIR spectroscopy, and X-ray fluorescence. *Remote Sensing*, *14*(19), 4823. https://doi.org/10.3390/rs14194823

Ramirez-Lopez, L., Wadoux, A. M. J. C., Franceschini, M. H. D., Terra, F. S., Marques, K. P. P., Sayão, V. M., & Demattê, J. A. M. (2018). Robust soil mapping at the farm scale with vis–NIR spectroscopy. *European Journal of Soil Science*, *70*(2), 378–393. https://doi.org/10.1111/ejss.12752

Rasche, F., Marhan, S., Berner, D., Keil, D., Kandeler, E., & Cadisch, G. (2013). midDRIFTS-based partial least square regression analysis allows predicting microbial biomass, enzyme activities and 16S rRNA gene abundance in soils of temperate grasslands. *Soil Biology & Biochemistry*, *57*, 504–512. https://doi.org/10.1016/j.soilbio.2012.09.030

Reeves, J. B., McCarty, G. W., & Hively, W. D. (2010). Mid-versus near-infrared spectroscopy for on-site analysis of soil. *Proximal Soil Sensing*, *158*, 133–142. https://doi.org/10.1016/j.geoderma.2009.04.005

Rinnan, Å., Van Den Berg, F., & Engelsen, S. B. (2009). Review of the most common pre-processing techniques for near-infrared spectra. *Trends in Analytical Chemistry*, *28*(10), 1201–1222. https://doi.org/10.1016/j.trac.2009.07.007

Romero, D. J., Ben-Dor, E., Demattê, J. A. M., Souza, A. B., Vicente, L. D., Tavares, T. T., Martello, M., Strabeli, T. F., Barros, P. P. S., Fiorio, P. R., Gallo, B. C., Sato, M. V., & Eitelwein, M. T. (2018). Internal soil standard method for the Brazilian soil spectral library: Performance and proximate analysis. *Geoderma*, *312*, 95–103. https://doi.org/10.1016/j.geoderma.2017.09.014

Rosin, N. A., Dematte, J. A., Leite, M. C. A., de Carvalho, H. W. P., Costa, A. C., Greschuk, L. T., Curi, N., & Silva, S. H. G. (2022). The fundamental of the effects of water, organic matter, and iron forms on the pXRF information in soil analyses. *Catena*, *210*, 105868. https://doi.org/10.1016/j.catena.2021.105868

Rosin, N. A., Demattê, J. A., Poppiel, R. R., Silvero, N. E., Rodriguez-Albarracin, H. S., Rosas, J. T. F., Greschuk, L. T., & Fernandes, K. (2023). Mapping Brazilian soil mineralogy using proximal and remote sensing data. *Geoderma*, *432*, 116413. https://doi.org/10.1016/j.geoderma.2023.116413

Sanderman, J., Gholizadeh, A., Pittaki-Chrysodonta, Z., Huang, J., Safanelli, J. L., & Ferguson, R. (2023). Transferability of a large mid-infrared soil spectral library between two Fourier-transform infrared spectrometers. *Soil Science Society of America Journal*, *87*(3), 586–599. https://doi.org/10.1002/saj2.20513

Sanderman, J., Savage, K., & Dangal, S. R. (2020). Mid-infrared spectroscopy for prediction of soil health indicators in the United States. *Soil Science Society of America Journal*, *84*(1), 251–261. https://doi.org/10.1002/saj2.20009

Santos, U. J., Demattê, J. A. M., Menezes, R. S. C., Dotto, A. C., Guimarães, C. C. B., Alves, B. J. R., Primo, D. C., & Sampaio, E. V. S. B. (2020). Predicting carbon and nitrogen by visible near-infrared (Vis-NIR) and mid-infrared (MIR) spectroscopy in soils of Northeast Brazil. *Geoderma Regional*, *23*(2020), e00333. https://doi.org/10.1016/j.geodrs.2020.e00333

Scheinost, A. C., Chavernas, A., Barron, V., & Torrent, J. (1998). Use and limitations of second-derivative diffuse reflectance spectroscopy in the visible to near-infrared range to identify and quantify Fe oxide minerals in soils. *Clays and Clay Minerals*, *46*, 528–536. https://doi.org/10.1346/CCMN.1998.0460506

Seidel, M., Vohland, M., Greenberg, I., Ludwig, B., Ortner, M., Thiele-Bruhn, S., & Hutengs, C. (2022). Soil moisture effects on predictive VNIR and MIR modeling of soil organic carbon and clay content. *Geoderma*, *427*, 116103. https://doi.org/10.1016/j.geoderma.2022.116103

Seybold, C. A., Ferguson, R., Wysocki, D., Bailey, S., Anderson, J., Nester, B., Schoeneberger, P., Wills, S., Libohova, Z., Hoover, D., & Thomas, P. (2019). Application of mid-infrared spectroscopy in soil survey. *Soil Science Society of America Journal*, *83*(6), 1746–1759. https://doi.org/10.2136/sssaj2019.06.0205

Sharma, A., Weindorf, D. C., Man, T., Aldabaa, A. A. A., & Chakraborty, S. (2014). Characterizing soils via portable X-ray fluorescence spectrometer: 3. Soil reaction (pH). *Geoderma*, *232*, 141–147. https://doi.org/10.1016/j.geoderma.2014.05.005

Shi, X., Song, J., Wang, H., Lv, X., Zhu, Y., Zhang, W., Bu, W., & Zeng, L. (2023). Improving soil organic matter estimation accuracy by combining optimal spectral preprocessing and feature selection methods based on pXRF and vis-NIR data fusion. *Geoderma*, *430*, 116301. https://doi.org/10.1016/j.geoderma.2022.116301

Silva, S. H. G., Ribeiro, B. T., Guerra, M. B. B., de Carvalho, H. W. P., Lopes, G., Carvalho, G. S., Guilherme, L. R. G., Resende, M., Mancini, M., Curi, N., Rafael, R. B. A., Cardelli, V., Cocco, S., Corti, G., Chakraborty, S., Li, B., & Weindorf, D. C. (2021). pXRF in tropical soils: Methodology, applications, achievements and challenges. *Advances in Agronomy*, *167*, 1–62. https://doi.org/10.1016/bs.agron.2020.12.001

Silva, S. H. G., Weindorf, D. C., Pinto, L. C., Faria, W. M., Junior, F. W. A., Gomide, L. R., Mello, J. M., Junior, F. W. A., Souza, I. A., Teixeria, A. F. S., Guilherme, L. R. G., & Curi, N. (2020). Soil texture prediction in tropical soils: A portable X-ray fluorescence spectrometry approach. *Geoderma*, *362*, 114136. https://doi.org/10.1016/j.geoderma.2019.114136

Silvero, N. E. Q., Di Raimo, L. A. D. L., Pereira, G. S., de Magalhães, L. P., Terra, F. D. S., Dassan, M. A. A., Salazar, D. F. U., & Demattê, J. A. M. (2020). Effects of water, organic matter, and iron forms in mid-IR spectra of soils: Assessments from laboratory to satellite-simulated data. *Geoderma*, *375*, 114480. https://doi.org/10.1016/j.geoderma.2020.114480

Soil Survey Staff. (2014). *Keys to soil taxonomy* (12th ed.). USDA-NRCS.

Sonmez, S., Buyuktas, D., Okturen, F., & Citak, S. (2008). Assessment of different soil to water ratios (1:1, 1:2.5, 1:5) in soil salinity studies. *Geoderma*, *144*(1–2), 361–369. https://doi.org/10.1016/j.geoderma.2007.12.005

Sørensen, L. K., & Dalsgaard, S. (2005). Determination of clay and other soil properties by near infrared spectroscopy. *Soil Science Society of America Journal*, *69*(1), 159–167. https://doi.org/10.2136/sssaj2005.0159

Soriano-Disla, J. M., Janik, L. J., Viscarra Rossel, R. A., Macdonald, L. M., & McLaughlin, M. J. (2014). The performance of visible, near-, and mid-infrared reflectance spectroscopy for prediction of soil physical, chemical, and biological properties. *Applied Spectroscopy Reviews*, *49*(2), 139–186. https://doi.org/10.1080/05704928.2013.811081

Stark, E. W. (1988). Calibration methods for NIRS analysis. In C. S. Creaser, & A. M. C. Davies (Eds.), *Analytical applications of spectroscopy* (pp. 21–34). Royal Society of Chemistry.

Stevenson, A., Hartemink, A. E., & Zhang, Y. (2023). Measuring sand content using sedimentation, spectroscopy, and laser diffraction. *Geoderma*, *429*, 116268. https://doi.org/10.1016/j.geoderma.2022.116268

Sun, W., Li, X., & Niu, B. (2018). Prediction of soil organic carbon in a coal mining area by Vis-NIR spectroscopy. *PLoS ONE*, *13*(4), e0196198. https://doi.org/10.1371/journal.pone.0196198

Szabolcs, I. (1994). The concept of soil resilience. In D. Greenland, & I. Szabolcs (Eds.), *Soil resilience and sustainable land use* (pp. 33–39). CAB International.

Tang, Y., Jones, E., & Minasny, B. (2020). Evaluating low-cost portable near infrared sensors for rapid analysis of soils from South Eastern Australia. *Geoderma Regional*, *20*, e00240. https://doi.org/10.1016/j.geodrs.2019.e00240

Tavares, T. R., Molin, J. P., Nunes, L. C., Alves, E. E. N., Melquiades, F. L., de Carvalho, H. W. P., & Mouazen, A. M. (2020). Effect of X-ray tube configuration on measurement of key soil fertility attributes with XRF. *Remote Sensing*, *12*(6), 963. https://doi.org/10.3390/rs12060963

Terra, F. S., Demattê, J. A., & Viscarra Rossel, R. A. (2015). Spectral libraries for quantitative analyses of tropical Brazilian soils: Comparing vis–NIR and mid-IR reflectance data. *Geoderma*, *255*, 81–93. https://doi.org/10.1016/j.geoderma.2015.04.017

Terra, F. S., Rossel, R. A. V., & Demattê, J. A. (2019). Spectral fusion by Outer Product Analysis (OPA) to improve predictions of soil organic C. *Geoderma*, *335*, 35–46. https://doi.org/10.1016/j.geoderma.2018.08.005

Tian, Y., Zhang, J., Yao, X., Cao, W., & Zhu, Y. (2013). Laboratory assessment of three quantitative methods for estimating the organic matter content of soils in China based on visible/near-infrared reflectance spectra. *Geoderma*, *202*, 161–170. https://doi.org/10.1016/j.geoderma.2013.03.018

Tsimpouris, E., Tsakiridis, N. L., & Theocharis, J. B. (2021). Using autoencoders to compress soil VNIR–SWIR spectra for more robust prediction of soil properties. *Geoderma*, *393*, 114967. https://doi.org/10.1016/j.geoderma.2021.114967

van Leeuwen, C. C., Mulder, V. L., Batjes, N. H., & Heuvelink, G. B. (2024). Effect of measurement error in wet chemistry soil data on the calibration and model performance of pedotransfer functions. *Geoderma*, *442*, 116762. https://doi.org/10.1016/j.geoderma.2023.116762

Vasques, G. M., Demattê, J. A. M., Viscarra Rossel, R. A., Ramírez-López, L., & Terra, F. S. (2014). Soil classification using visible/near-infrared diffuse reflectance spectra from multiple depths. *Geoderma*, *223–225*, 73–78. https://doi.org/10.1016/j.geoderma.2014.01.019

Vasques, G. M., Demattê, J. A. M., Viscarra Rossel, R. A., Ramírez López, L., Terra, F. D. S., Rizzo, R., & De Souza Filho, C. R. (2015). Integrating geospatial and multi-depth laboratory spectral data for mapping soil classes in a geologically complex area in southeastern Brazil. *European Journal of Soil Science*, *66*(4), 767–779. https://doi.org/10.1111/ejss.12255

Vasques, G. M., Grunwald, S., & Sickman, J. O. (2008). Comparison of multivariate methods for inferential modeling of soil carbon using visible/near-infrared spectra. *Geoderma*, *146*(1–2), 14–25. https://doi.org/10.1016/j.geoderma.2008.04.007

Viscarra Rossel, R. A., & Behrens, T. (2010). Using data mining to model and interpret soil diffuse reflectance spectra. *Geoderma*, *158*(1–2), 46–54. https://doi.org/10.1016/j.geoderma.2009.12.025

Viscarra Rossel, R. A., Behrens, T., Ben-Dor, E., Brownd, D. J., Demattê, J. A. M., Shepherd, K. D., Shi, Z., Stenberg, B., Stevens, A., Adamchukj, V., Aïchi, H., Barthès, B. G., Bartholomeus, H. M., Bayer, A. D., Bernoux, M., Böttcher, K., Brodský, L., Du, C. W., Chappell, A., … Ji, W. (2016). A global spectral library to characterize the world's soil. *Earth-Science Reviews*, *155*, 198–230. https://doi.org/10.1016/j.earscirev.2016.01.012

Viscarra Rossel, R. A., Cattle, S. R., Ortega, A., & Fouad, Y. (2009). In situ measurements of soil colour, mineral composition and clay content by vis–NIR spectroscopy. *Geoderma*, *150*(3–4), 253–266. https://doi.org/10.1016/j.geoderma.2009.01.025

Viscarra Rossel, R. A., & Lark, R. M. (2009). Improved analysis and modelling of soil diffuse reflectance spectra using wavelets. *European Journal of Soil Science*, *60*(3), 453–464. https://doi.org/10.1111/j.1365-2389.2009.01121.x

Viscarra Rossel, R. A., Walvoort, D. J. J., McBratney, A. B., Janik, L. J., & Skjemstad, J. O. (2006). Visible, near infrared, mid infrared or combined diffuse reflectance spectroscopy for simultaneous assessment of various soil properties. *Geoderma*, *131*(1–2), 59–75. https://doi.org/10.1016/j.geoderma.2005.03.007

Wang, D., Chakraborty, S., Weindorf, D. C., Li, B., Sharma, A., Paul, S., & Ali, M. N. (2015). Synthesized use of VisNIR DRS and PXRF for soil characterization: Total carbon and total nitrogen. *Geoderma*, *243*, 157–167. https://doi.org/10.1016/j.geoderma.2014.12.011

Wang, J., Cui, L., Gao, W., Shi, T., Chen, Y., & Gao, Y. (2014). Prediction of low heavy metal concentrations in agricultural soils using visible and near-infrared reflectance spectroscopy. *Geoderma*, *216*, 1–9. https://doi.org/10.1016/j.geoderma.2013.10.024

Weerasekara, M., Hartemink, A. E., Zhang, Y., & Stevenson, A. (2024). Spectral signatures of soil horizons and soil orders from Wisconsin. *Soil Science Society of America Journal*, *88*, 2013–2030. https://doi.org/10.1002/saj2.20766

Weindorf, D. C., Chakraborty, S., Abdalsatar, A., Aldabaa, A., Paulette, L., Corti, G., Cocco, S., Micherli, E., Wang, D., Li, B., Man, T., Sharma, A., & Person, T. (2015). Lithologic discontinuity assessment in soils via portable X-ray fluorescence spectrometry and visible near-infrared diffuse reflectance spectroscopy. *Soil Science Society of America Journal*, *79*(6), 1704–1716. https://doi.org/10.2136/sssaj2015.04.0160

Weindorf, D. C., Zhu, Y., McDaniel, P., Valerio, M., Lynn, L., Michaelson, G., Clark, M., & Ping, C. L. (2012). Characterizing soils via portable X-ray fluorescence spectrometer: 2. Spodic and

Albic horizons. *Geoderma*, *189*, 268–277. https://doi.org/10.1016/j.geoderma.2012.06.034

Wijewardane, N. K., Ge, Y., Wills, S., & Libohova, Z. (2018). Predicting physical and chemical properties of US soils with a mid-infrared reflectance spectral library. *Soil Science Society of America Journal*, *82*(3), 722–731. https://doi.org/10.2136/sssaj2017.10.0361

Wijewardane, N. K., Ge, Y., Wills, S., & Loecke, T. (2016). Prediction of soil carbon in the conterminous United States: Visible and near infrared reflectance spectroscopy analysis of the rapid carbon assessment project. *Soil Science Society of America Journal*, *80*(4), 973–982. https://doi.org/10.2136/sssaj2016.02.0052

Xian-Li, X. I. E., Xian-Zhang, P., & Bo, S. (2012). Visible and near-infrared diffuse reflectance spectroscopy for prediction of soil properties near a copper smelter. *Pedosphere*, *22*(3), 351–366. https://doi.org/10.1016/S1002-0160(12)60022-8

Xie, X. L., & Li, A. B. (2018). Identification of soil profile classes using depth-weighted visible–near-infrared spectral reflectance. *Geoderma*, *325*, 90–101. https://doi.org/10.1016/j.geoderma.2018.03.029

Xu, H., Xu, D., Chen, S., Ma, W., & Shi, Z. (2020). Rapid determination of soil class based on visible-near infrared, mid-infrared spectroscopy and data fusion. *Remote Sensing*, *12*(9), 1512. https://doi.org/10.3390/rs12091512

Young, I., & Crawford, J. (2004). Interactions and self-organisation in the soil-microbe complex. *Science*, *304*, 1634–1637. https://doi.org/10.1126/science.1097394

Zhang, Y., Freedman, Z. B., Hartemink, A. E., Whitman, T., & Huang, J. (2022). Characterizing soil microbial properties using MIR spectra across 12 ecoclimatic zones (NEON sites). *Geoderma*, *409*, 115647. https://doi.org/10.1016/j.geoderma.2021.115647

Zhang, Y., & Hartemink, A. E. (2020). Data fusion of vis–NIR and PXRF spectra to predict soil physical and chemical properties. *European Journal of Soil Science*, *71*(3), 316–333. https://doi.org/10.1111/ejss.12875

Zhang, Y., & Hartemink, A. E. (2021). Quantifying short-range variation of soil texture and total carbon of a 330-ha farm. *Catena*, *201*, 105200. https://doi.org/10.1016/j.catena.2021.105200

Zhang, Y., Hartemink, A. E., & Huang, J. (2021). Spectral signatures of soil horizons and soil orders—An exploratory study of 270 soil profiles. *Geoderma*, *389*, 114961. https://doi.org/10.1016/j.geoderma.2021.114961

Zhao, D., Arshad, M., Li, N., & Triantafilis, J. (2021). Predicting soil physical and chemical properties using vis-NIR in Australian cotton areas. *Catena*, *196*, 104938. https://doi.org/10.1016/j.catena.2020.104938

Zhu, Y., Weindorf, D. C., & Zhang, W. (2011). Characterizing soils using a portable X-ray fluorescence spectrometer: 1. Soil texture. *Geoderma*, *167*, 167–177. https://doi.org/10.1016/j.geoderma.2011.08.010

SUPPORTING INFORMATION

Additional supporting information can be found online in the Supporting Information section at the end of this article.

How to cite this article: Gozukara, G., Hartemink, A. E., Huang, J., & Demattê, J. A. M. (2025). Prediction accuracy of pXRF, MIR, and Vis-NIR spectra for soil properties—A review. *Soil Science Society of America Journal*, *89*, e70028. https://doi.org/10.1002/saj2.70028